JAAS
Journal of Analytical Atomic Spectrometry

Accepted Manuscript

This article can be cited before page numbers have been issued, to do this please use: A. Hassler, E. E. Lindroos, L. Yang, A. Dosseto, F. Dux, Z. Mester, K. Britton and C. P. Bataille, *J. Anal. At. Spectrom.*, 2026, DOI: 10.1039/D6JA00007J.

ROYAL SOCIETY OF CHEMISTRY

rsc.li/jaas

View Article Online
DOI: 10.1039/D6JA00007J

Advances in Calcium Isotope Purification and Analysis Using Cutting-Edge Signal Amplifiers for Matrix-Diverse Reference Materials

Authors

Auguste Hassler[1,2,3,*], Eve E. Lindroos[1,4], Lu Yang[3], Anthony Dosseto[5], Florian Dux[5], Zoltan Mester[3], Kate Britton[2,‡], Clément P. Bataille[1,6,‡]

Affiliation

1: Department of Earth and Environmental Sciences, University of Ottawa, Advanced Research Complex building, 25 Templeton St., K1N 7N9, Ottawa, ON, Canada

2: Department of Archaeology, University of Aberdeen, St. Mary's Elphinstone Road, AB24 3UF Aberdeen, Scotland, UK

3: Metrology Research Centre, National Research Council Canada, 1200 Montreal Rd., Ottawa, Ontario, Canada K1A 0R6.

4: Géosciences Environnement Toulouse, Observatoire Midi Pyrénées, CNRS/UMR 5563, 14 avenue Edouard Belin, 31400 Toulouse, France

5: Wollongong Isotope Geochronology Laboratory, Environmental Futures, School of Science, University of Wollongong, NSW, 2522, Australia

6: Department of Forestry and Natural Resources, Purdue University, 715 W. State Street, West Lafayette, IN, 47907, USA

*: corresponding author

‡: These senior authors contributed equally

ORCID

Auguste Hassler: 0000-0003-3004-4680

Eve E. Lindroos: 0009-0004-8314-6685

Lu Yang: 0000-0002-6896-8603

Anthony Dosseto: 0000-0002-3575-0106

Florian Dux: 0000-0002-3275-710X

Zoltan Mester: 0000-0002-2377-2615

Kate Britton: 0000-0002-9478-5966

Clément Bataille: 0000-0001-8625-4658

View Article Online
DOI: 10.1039/D6JA00007J

Key words

$10^{13}\Omega$, interference, matrix effect, biological, precision, accuracy, strontium, Sr, Ca, ICPMS, chromatography

Abstract

Stable calcium (Ca) isotopes are increasingly applied across geosciences, medical sciences, ecology, paleontology, and archaeology. However, the deployment speed of Ca isotope applications worldwide is hampered by three major challenges: 1) the necessity for complex Ca purification procedures prior to analysis; 2) expensive instrumentation (typically TIMS or ICP-MS) requiring specific configurations and fine-tuning to generate reliable data; and 3) the exhaustion of some of the most widely used reference materials for cross-laboratory comparisons. This study presents methodological advances aimed at lifting some of these barriers. First, existing chromatography methods for purifying Ca were refined by developing a branching procedure based on commercially available labware to allow faster method transfer and to minimize resin and reagent consumption for a variety of sample matrices. These adjustments drastically improved strontium (Sr) separation from Ca, including for Sr-rich samples such as seawater. Second, the potential of $10^{13}\Omega$ Faraday cup amplifiers for improving Ca isotope measurements was explored. Results show improved precision in ^{43}Ca measurements under low ionic transmission configurations with $\delta^{43/42}Ca$ standard deviation value reduced by half. This expands the list of ICP-MS configurations capable of producing reliable Ca isotope measurements and delineates a path for less sample-destructive methods (i.e., lower Ca analytical requirements). These amplifiers also markedly enhanced the correction of Sr^{2+} interferences typically affecting Ca ion beams. In this configuration, accurate and precise Ca isotopic measurements were obtained without prior Sr removal for Sr/Ca concentration ratios up to 10^{-2}. Lastly, using these technical advancements, existing and new international certified reference materials (SRM1486, SRM1400, IAPSO, CACB-1, DOLT-5, DORM-5, TORT-3) were analyzed, complementing existing and out-of-stock standards of the Ca isotope toolbox, notably for Ca carbonate and marine soft tissues. Together, these advances open the door of Ca isotope research to more laboratories and pave the way for future developments and applications.

1. Introduction

Stable calcium (Ca) isotope geochemistry emerged in the late 1970s to investigate cosmological and geological fractionations [1,2] and then expanded into biological materials in the 1990s [3,4]. This triggered the development of new applications in (paleo-)ecology, archaeology, and biomedical sciences, supported by the deployment of commercially available instruments of thermal ionization mass spectrometry (TIMS) and multi-collector inductively coupled plasma mass spectrometry (MC-ICP-MS) [5–7]. Despite this growth, Ca isotope analysis remains confined to a few specialized laboratories due to multiple cross-disciplinary challenges and high upfront and maintenance costs for the instrumentation [5,6]. In this context, while maintaining efforts for ever lower sampling requirements and improved measurement precision and accuracy, it is also important to develop methods that help to open this field to new laboratories by, e.g., limiting or mutualizing up-front costs and simplifying laboratory operations.

With a few exceptions (e.g., laser ablation or chemically pure samples), Ca isotope measurements normally require prior separation of Ca from interfering elements. This purification is commonly done via column chromatography using specific resins, with two main trends coexisting in the recent

View Article Online
DOI: 10.1039/D6JA00007J

literature. First, the use of DGA resins from Eichrom, which offer interesting perspectives of time efficiency and low reagent use for Ca and Sr purification [8–18]. Second, the use of various combinations of AG® Bio-Rad and Sr Eichrom resins. This second approach benefits from the widespread adoption of AG® Bio-Rad and Sr Eichrom resins in geochemistry laboratories, owing to their central role in a variety of independent chromatography procedures (e.g., for Li, Mg, Fe, Cu, Zn, Sr, Pb, REE applications: [19–27]), including for achieving the isolation of multiple elements from a single aliquot (e.g., for Ca, Sr, Mg, K or Zn: [21,27,28]). This broad use facilitates the implementation of Ca isotope purification approach in laboratories with preexisting geochemistry backgrounds, equipment and workflows, while also permitting cost mutualization across research teams with different research objectives and easier integration within multi-proxy workflows. These considerations motivated our choice of the AG® Bio-Rad and Sr Eichrom resins approach for this project. However, both this approach and DGA based ones face a similar dilemma between building versatile procedures applicable to a wide range of sample types and their elemental matrices, versus building more sample specific procedures to optimize time and reagent use. To address this, we developed a branching procedure aiming to reconcile matrix versatility with time and reagent use efficiency.

Traditionally, Ca isotope compositions are analyzed via either TIMS or MC-ICP-MS [2,7,29,30], with MC-ICP-MS being generally favored for studying biological materials due to its higher sample throughput [7,8,26,30]. The recent development of low signal noise $10^{13}\Omega$ Faraday cup amplifiers (Thermo Fisher Scientific) allows to accurately and precisely measure low-intensity ion beams in the fA range, as previously demonstrated for isotopic systems other than Ca [31–33]. This opens up the possibility for better low-abundance isotope measurements (e.g., for ^{43}Ca) and for decreasing the amount of Ca required per analysis (i.e., less destructive sampling), without necessitating the implementation of desolvating systems (i.e., dry plasma), or large interface pump add-ons (permitting the use of high transmission cones in wet plasma, e.g., jet and X cones). This new class of amplifier creates the opportunity to revisit previously impractical configurations of MC-ICP-MS while further pushing the boundaries of analytical performance [7].

Ca isotopic compositions are conventionally expressed as δCa values in ‰ (e.g., $\delta^{44/42}Ca$, $\delta^{43/42}Ca$, and $\delta^{44/40}Ca$), defined as: $\delta^{X/Y}Ca$ (‰) = (($R^{X/Y}Ca_{sample}$ / $R^{X/Y}Ca_{standard}$) – 1) x 1000, where X and Y are two Ca isotopes and *R* is the corresponding isotope ratio for a given sample and the primary standard (classically a reference material). This arises from technological difficulties in measuring absolute isotopic compositions accurately and the need for inter-laboratory comparisons. The SRM915a Ca carbonate from NIST is the reference material which is the most commonly used as primary standard in Ca isotope geochemistry [2,7,34]. However, SRM915a has been out of stock since 2006, making this scale increasingly impractical by forcing laboratories to use other reference materials (previously calibrated against SRM915a) as intermediates to convert measurements to SRM915a-scaled δCa values, propagating additional measurement uncertainty in the process [2,35]. Moreover, using reference materials with elemental matrices similar to samples (as primary or secondary standards) is imperative for both chromatography and spectrometry quality control. These issues highlight the need for continued characterization of more Ca isotope reference materials [7].

This study addresses three core objectives within this context of technological developments and challenges. First, a versatile chromatography protocol designed to process diverse sample matrices (e.g., calcium carbonates, bioapatites, seawater and marine soft tissues) was developed, while optimizing resin and reagent efficiency, as well as ensuring high standards of labware accessibility to facilitate method transfer and reproducibility. This approach involves a branching 1- to 3-step Ca and Sr purification procedure, building on established methods using AG® Bio-Rad and Sr Eichrom resins [20–22,36]. Notably, here, different Sr resin grades (50-100 µm versus 100-150 µm particle size) are tested to compare Ca-Sr separation performances for neutralizing Sr contaminations, a common obstacle for accurate Ca isotope measurement by ICP-MS [20,26,37,38].

View Article Online
DOI: 10.1039/D6JA00007J

Second, a broadening of instrumental configurations available for Ca isotope analysis was sought, in order to open this field to more laboratories and foster interdisciplinary applications [5]. Specifically, the performance of $10^{13}\Omega$ Faraday cup amplifiers (Thermo Fisher Scientific) in reliably monitoring Ca isotopic fractionation mass dependency was evaluated under low ionic transmission conditions (i.e., wet plasma without large interface pump and high transmission cones), notably for quality control purposes. Low ionic transmission configurations can be particularly challenging in this aspect because this monitoring requires reliable measurements of $^{43}Ca^{+}$ signals, which have very low intensities due to this low transmission combined with the naturally low abundance of ^{43}Ca (0.135 %) [2,20,24]. Additionally, the potential of these amplifiers to improve Sr^{2+} corrections was explored, as Sr^{2+} beams (typically in the fA range) are one of the most significant interferences affecting Ca isotope measurements by MC-ICP-MS [20,26,37,38]. Within this low ionic transmission configuration, different amplifier configurations and acquisition parameters were tested in order to identify which could provide the best compromise between accuracy, precision, Ca consumption and acquisition time.

Finally, the suite of reference standards available to the Ca isotope community was expanded by cross-analyzing seven international reference materials with varied elemental matrices. These included commonly used standards of carbonated (bio)apatite (SRM1486 and SRM1400 from NIST), seawater (IAPSO from OSIL), and newly analyzed Ca carbonate (CACB-1 from NRC) and marine soft tissues (DOLT-5, DORM-5, TORT-3 from NRC)[39–42]. These reference materials also served to validate the robustness of the chromatography and spectrometry procedures proposed here.

2. Materials and methods

2.1. Labware and reagents

Ultrapure water (resistivity ≥ 18.2 MΩ.cm at 25°C, milli-Q, Millipore system) was used for all cleanings and dilutions. ACS grade hydrochloric acid (HCl) and nitric acid (HNO_3) were used for initial labware cleaning steps, whereas HCl and HNO_3 of trace metal grade (TMG), or ACS grade distilled in-house with a Savilex DST-1000 Acid Purification System, were used for final labware cleaning and all steps involving direct sample contact. Commercially purchased TMG and in-house distilled ACS grade acids delivered similar levels of trace element concentrations. They were used interchangeably throughout this work and simply referred to as TMG thereafter. Labware used in this study includes PFA, PTFE, polypropylene and polyethylene vials and consumables, the specifications and cleaning procedures of which are detailed in Supplementary information. Sample preparation steps were carried out in a dust-free environment within the University of Ottawa Geochemistry Core Facility clean laboratory.

2.2. International and in-house standards

Seven international certified reference materials (CRMs) were processed to ensure precise and accurate Ca isotope measurements across diverse elemental matrices. These were used as secondary standards and are referred to as such, or simply as 'samples' in this manuscript. These materials include cow bone reference materials SRM1486 (steamed and blended) and SRM1400 (ashed and blended) from the US National Institute of Standards and Technology (NIST), IAPSO seawater from Ocean Scientific International Ltd (OSIL), the Ca carbonate CACB-1 and marine soft tissues DOLT-5 dogfish liver (*Squalus acanthias*), DORM-5 fish protein, and TORT-3 lobster hepatopancreas reference materials, all four from the National Research Council of Canada (NRC) [39–42]. Every chromatography load of these reference materials represented a mass of approximately 0.5 mg for SRM1486 and SRM1400, 0.125 mg for CACB-1, 91 mg for DOLT-5, 25 mg for DORM-5, 19 mg for TORT-3, and 121 mg for IAPSO, representing between 40 to 150 µg of Ca. Additionally, a solution of Ca plasma standard solution (10,000 µg/ml, Specpure, Product no: 014407, Lot no: 1359261, Thermo Scientific), referred to as "alpha-Ottawa" served as the in-house bracketing standard during Ca isotope measurements and

as the primary standard for δCa. In this paper, the term 'δCa value' refers indiscriminately to both $\delta^{44/42}Ca$ and $\delta^{43/42}Ca$ values (and occasionally to $\delta^{44/40}Ca$ values when discussing the literature).

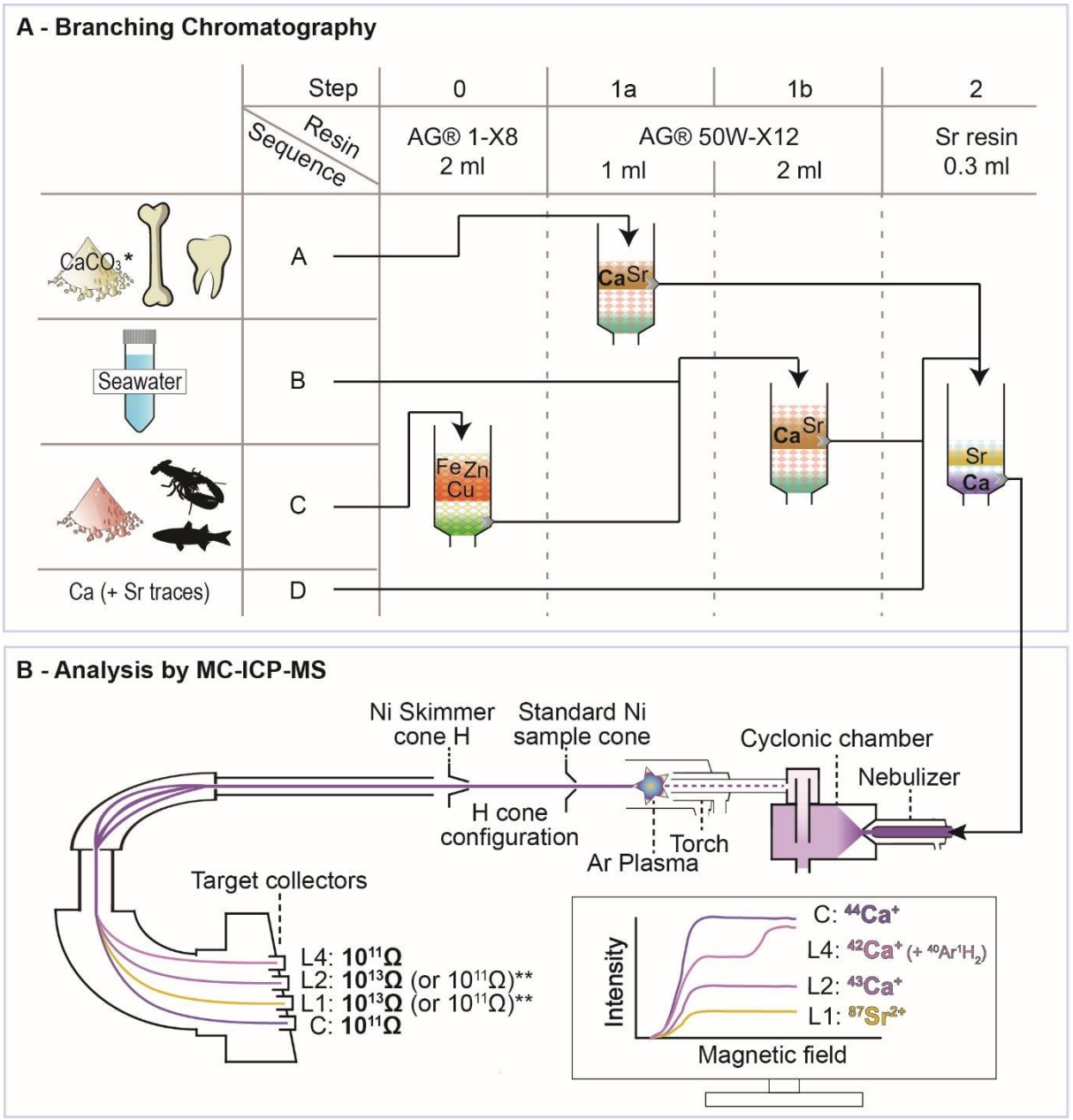

Figure 1: *Analytical workflow summary. Part A - outlines the proposed branching chromatography procedure necessary prior to Ca isotope analyses, with its four distinct sequences based on sample composition. Sequence A is adapted to Ca carbonates and bioapatites, sequence B to seawater, sequence C to soft tissues (notably from marine origin) and sequence D to relatively pure Ca solutions. Appropriate Sr interference correction can allow for the chromatography of step 2 to be skipped in certain conditions (or all chromatography for sequence D), as critically discussed later in this manuscript. *: Depending on initial purity, Ca carbonates can also be reliably purified through sequence D. Part B – outlines the default instrumental configuration, Faraday cup configuration, and amplifier pairing adopted in this study for Ca isotope analyses on MC-ICPM-MS, resulting in low ionic transmission but high signal amplification of the lowest intensity ion beams (i.e., $10^{13}\Omega$ amplifiers were paired with L1 and L2 cups for $^{43}Ca^{+}$ and $^{87}Sr^{2+}$ beams, respectively). **: For comparisons and certain calibration steps (e.g., amplifier gain calibration) L1 and L2 cups were occasionally paired with conventional $10^{11}\Omega$ amplifiers. Graphic design inspired by [43].*

2.3. Sample preparation

Samples with limited organic content (SRM1400, SRM1486, CACB-1, IAPSO) were digested in 2 ml of 15 M HNO_3 on a hot plate at 120°C for at least 2 hours. Samples with more abundant organic content

View Article Online
DOI: 10.1039/D6JA00007J

(DOLT-5, DORM-5, TORT-3) underwent microwave-assisted digestion with 2 ml of 15 M HNO_3 (20-minute ramp and 30-minute hold at 250°C, 40 bar pressure, Multiwave 7000, Anton Paar). All digests were evaporated to dryness, redissolved in 10 M HCl, and evaporated again before being conditioned for chromatography.

Table 1: *Chromatography steps for matrix elution and Ca-Sr separation. Greyed out stages with bold font indicate collection stages allowing quantitative Ca recovery. Quantitative recovery of Sr is also possible providing the addition of an optional elution stage for steps 1a and 1b, as detailed in the table. The sequencing of these chromatography steps is outlined in Figure 1A and detailed in Table 2. Resin cleaning and recycling procedures are detailed in Supplementary information.*

Step 0. Fe, Cu and Zn elimination (AG® 1-X8, 100-200 mesh, 2 ml)	Reagent	Volume (ml)
Conditioning	HCl 6 M	8
Loading	**HCl 6 M**	**3.5**
Elution (Ca, matrix)	**HCl 6 M**	**5.5**
Elution (Fe, Cu, Zn)	HNO_3 0.5 M	10
Terminal wash	HNO_3 0.5 M	10

Step 1a. Core matrix elution (AG® 50W-X12, 200-400 mesh, 1 ml)	Reagent	Volume (ml)
Conditioning	HCl 1 M	4
Loading	HCl 1 M	0.1
Elution (matrix)	HCl 1 M	22.9
Elution (Ca, Sr)	**HCl 6 M**	**6**
Optional - Elution (Sr remainder)	HCl 6 M	5
Terminal wash	HCl 6 M	10

Step 1b. Core matrix elution (AG® 50W-X12, 200-400 mesh, 2 ml)	Reagent	Volume (ml)
Conditioning	HCl 1 M	8
Loading	HCl 1 M	0.5
Elution (matrix)	HCl 1 M	59.5
Elution (Ca, Sr)	**HCl 6 M**	**13**
Optional - Elution (Sr remainder)	HCl 6 M	5
Terminal wash	HCl 6 M	10

Step 2. Sr elimination (Sr resin, 50-100 µm particle size, 0.3 ml)	Reagent	Volume (ml)
Conditioning	HNO_3 3 M	4
Loading	**HNO_3 3 M**	**0.3**
Elution (Ca)	**HNO_3 3 M**	**3.2**
Elution (Sr)	HNO_3 0.005 M	7
Terminal wash	HNO_3 0.005 M	4

2.4. Chromatography procedures

The chromatography workflow, adapted from previous studies [20–22,36] and outlined in Figure 1A, used Poly-Prep® Columns (Bio-Rad) for initial steps with AG® 1-X8 (100-200 mesh) and AG® 50W-X12 (200-400 mesh) resins (Bio-Rad), followed by final Sr-Ca separation with Eichrom Sr resin packed in repurposed 5 ml transfer pipettes. In this work, the use of the Eichrom Sr resin 50-100 µm particle size grade was explored in order to test for possible improvement in Sr-Ca separation compared to the more traditionally used 100-150 µm particle size grade. Beyond these preliminary tests, the 50-100 µm particle size grade has been the standard Sr resin grade used throughout this work. Resin preparation and column specifications are detailed in Supplementary information. Depending on sample matrix, a branching procedure of 1-3 steps was applied (Figure 1A, Table 1), resulting in 4 sequence types (Figure 1A, Table 2). This includes sequence A, where Ca-abundant samples like bioapatite and Ca carbonate (SRM1400, SRM1486, CACB-1) are processed through a 2-step chromatography with 1 ml of AG® 50W-X12 and 0.3 ml of Sr resin (steps 1a → 2; Table 1, Table 2). Sequence B, for samples with lower Ca/matrix ratio and high Mg content such as seawater, consisting

View Article Online
DOI: 10.1039/D6JA00007J

of a modified 2-step chromatography with 2 ml of AG® 50W-X12 and 0.3 ml of Sr resin (steps 1b → 2; Table 1, Table 2). Sequence C, where soft tissues (DOLT-5, DORM-5, TORT-3), characterized by low Ca/matrix ratios and high Fe, Cu and Zn content, require a 3-step chromatography starting with 2 ml of AG® 1-X8 resin to remove Fe, Cu and Zn before following the same steps as sequence B (steps 0 → 1b → 2; Table 1, Table 2). Although Fe, Cu and Zn are not prone to create isobaric interferences on Ca isotopes, high abundances of these elements can cause matrix effects indirectly affecting measurements (see discussion on doping experiments). This extra step also reduces the ionic load to prevent resin saturation and shifts in elution profiles. Finally, sequence D whereby pre-purified Ca solutions (e.g., alpha-Ottawa) are processed through a simple 1-step chromatography with 0.3 ml of Sr resin to remove residual Sr (step 2; Table 1, Table 2). The assignment of Ca carbonates to sequence A and the necessity of step 2 depends on the instrumental configuration for Ca isotope analyses and is critically discussed later in the text. To eliminate residual esters, every solution collected after step 2 (i.e., Sr-Ca separation with Sr resin) underwent a one-hour digestion with 0.5 ml of 15 M HNO_3 (TMG) on a hot plate at 120°C after evaporation to dryness. Where quantitative Sr collection from the same aliquot is intended, an optional elution stage can be added to steps 1a and 1b (see Table 1). Additional details of chromatography design are provided in Supplementary information.

The reliability of the chromatography procedures was assessed by monitoring elution profiles and evaluating Ca yields (outlined in Figure 2). To further verify the absence of chromatography-induced fractionation, matrix solutions collected from reference materials outside of the Ca collection stages were spiked with 50 µg of Ca from the alpha-Ottawa standard, re-processed through the same chromatography sequences, and analyzed. These test solutions are hereafter referred to as Ca-spiked matrix solutions.

Table 2: *Branching chromatography sequencing based on sample elemental content, necessary for Ca purification prior to Ca isotope analysis as outlined in Figure 1A. Step 2 can be made unnecessary for all sequences when appropriate Sr interference correction is performed (critically discussed later in the text). *: Alternatively, pure (or near pure) Ca carbonates (such as CACB-1) can also be satisfactorily purified through a simple 1-step sequence D.*

Procedure	Criteria	Examples	Step			
			0	1a	1b	2
Sequence type A	High Ca/matrix ratio	Bones (SRM1486, SRM1400), Ca carbonates (CACB-1)*, tooth enamel, dentin		V		V
Sequence type B	Low Ca/matrix ratio, high Mg, Mn or K content	Seawater (IAPSO)			V	V
Sequence type C	Low to very low Ca/matrix ratio, high Mg, Mn or K content, high Fe, Cu and Zn content	Soft tissues (DOLT-5, DORM-5, TORT-3)	V		V	V
Sequence type D	Pre-purified Ca solution, very high Ca/matrix ratio	Specpure Ca solution (alpha-Ottawa)				V

2.5. Elemental measurements

Elution profiles and yield measurements were performed using ICP-OES (Agilent 5110 SDV) and Q-ICP-MS (Agilent 8800 QQQ and Agilent 8900 QQQ) at the University of Ottawa's geochemistry laboratory (Advanced Research Complex). For elemental measurements, collected aliquots were evaporated to dryness, redissolved in 0.5 M HNO_3 (TMG), and spiked to concentrations of either 1 ppm scandium (for ICP-OES) or 2 ppb indium (for Q-ICP-MS) as internal standards for drift correction.

View Article Online
DOI: 10.1039/D6JA00007J

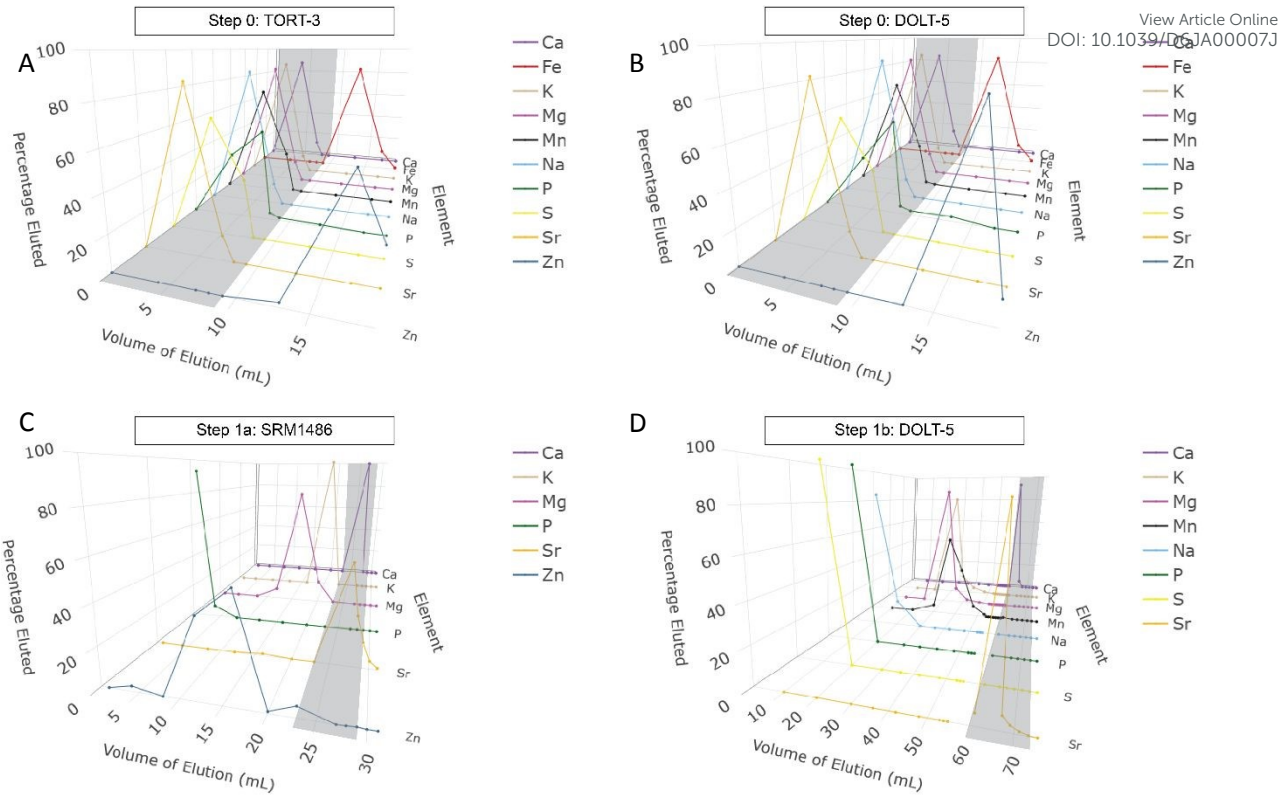

Figure 2: *Subset of elution profiles for chromatography steps 0 (A, TORT-3; B, DOLT-5), 1a (C, SRM1486) and 1b (D, DOLT-5). This show quantitative Ca recovery (100 % within measurement precision) during Ca collection phases (grey areas) and successful separation from matrix elements, with the exception of Sr which is separated from Ca during chromatography step 2 (quantitative recovery is achieved too). Collecting an extra 5 ml of 6M HCl after Ca collection steps in grey for steps 1a and 1b allow for a quantitative recovery of Sr* (Table 1).

2.6. Ca isotope analyses

2.6.1. Instrumentation

Ca isotope measurements were performed on two Neptune Plus MC-ICP-MS instruments (Thermo-Fisher), including one at the Metrology Research Centre of the NRC (Ottawa, Canada) and the other at the Wollongong Isotope Geochronology Laboratory (WIGL), University of Wollongong (Wollongong, NSW, Australia). Most of the data was generated at the NRC, where different instrument configurations were tested (Figure 1B, Table 3), the main parameters of which are detailed below and in Supplementary information.

Samples analyzed at WIGL were prepared at the University of Ottawa using identical digestion and chromatography procedures (Figure 1A, Table 1, Table 2) and shipped to WIGL for analysis. The MC-ICP-MS configuration at WIGL has been described previously [18]: dry plasma with a Cetac Aridus II desolvating system, jet sample and X skimmer cones, medium mass resolution, all $10^{11}\Omega$ amplifiers and analyses performed in 0.05 M HNO_3 at 1.5 ppm Ca.

2.6.2. Introduction and cone system

For all NRC configurations, a PFA-50 MicroFlow nebulizer integrated with the SC-Micro DX autosampler (ESI) connected to a Quartz SSI Spray Chamber (ESI, ES-2101-2001) in wet plasma mode was used (Figure 1B). The primary cone set was a standard Ni sample cone (not jet) and Ni H skimmer cone (referred to as H configuration). A standard Ni sample and X skimmer cone configuration (referred to as X configuration) was also tested for comparison. These wet plasma configurations do not require a

View Article Online
DOI: 10.1039/D6JA00007J

large interface pump system (an optional instrumentation upgrade) and yield lower ionic transmission compared to other setups such as Ni jet sample and X skimmer cones in wet (e.g., [14]) or dry plasma modes (e.g., [20,24,26]). To compensate for this lower transmission, higher Ca concentrations in both samples and bracketing standards were used (Table 3), although the low sample flow rate of this configuration partially offsets the increased Ca consumption (20 µg of Ca allows for 4 replicated measurements with a sample and standard Ca concentration of 10 ppm). Samples were introduced as 2 % v/v HNO_3 (TMG) solutions, and Ca concentrations were matched to bracket standards within ±10 % to prevent concentration-dependent bias (Supplementary information). A conventional "hot plasma" setting with a RF power of 1200 W was used [24]. After initial plasma ignition, "warm up" and stabilization phase (1 to 3 hours), the plasma was maintained continuously ignited for hours to days (up to 5 days) for a succession of analytical sessions routinely lasting 1 to 15 hours each. Routine tuning parameters (inlet system, source lenses, zoom optics, central cup position) were optimized before analytical sessions to maximize signal intensity and stability (see Supplementary information).

Table 3: *Summary of screened ICP-MS configurations, acquisition parameters and their respective preliminary results. *: this configuration produced an unstable signal and high $\delta^{44/42}$Ca standard deviation (expressed as 2 SD in ‰ in the table), **: this configuration was adopted as the default method in this study (outlined in Figure 1B), ***: this configuration provided promising preliminary results in regard to δCa SD values but doubles the Ca needed per measurement.*

		Tested configurations										
General configuration		Neptune plus, Wet plasma, RF power = 1200 W, Medium resolution slit										
Skimmer cone		X	H									
Amplifier configuration (Faraday mode)		full 4x $10^{11}\Omega$ static	full 4x $10^{11}\Omega$ static	full 4x $10^{11}\Omega$ rotating		hybrid 2x $10^{11}\Omega$ (C, L4) - 2x $10^{13}\Omega$ (L1, L2)						
Signal acquisition method		40 x 2.097s	40 x 2.097s	4 x 5 x 4.194s	4 x 5 x 4.194s	30 x 4.194s	40 x 2.097s	30 x 4.194s	40 x 4.194s	20 x 8.388s	30 x 4.194s	30 x 4.194s
Total integration time (s)		83.88	83.88	83.88	83.88	125.8	83.88	125.8	167.8	167.8	125.8	125.8
Ca concentration (ppm)		10	10	10	20	5	10				15	20
Average intensity (in $10^{11}\Omega$ equivalent, 1 V = 10 pA)	**$^{44}Ca^+$**	5.73 V	1.34 V	0.97 V	1.85 V	0.54 V	0.99 to 1.47 V				1.34V	1.82 V
	$^{43}Ca^+$	0.36 V	0.08 V	0.06 V	0.11 V	0.03 V	0.06 to 0.09 V				0.08 V	0.11 V
	$^{42}Ca^+$	1.67 V	0.38 V	0.28 V	0.53 V	0.15 V	0.28 to 0.42 V				0.38 V	0.52 V
Average 2 SD of δCa (‰)	**44/42**	0.45	0.19	0.21	0.17	0.22	0.24	0.12	0.09	0.10	0.09	0.07
	43/42	0.24	0.42	0.50	0.32	0.33	0.46	0.21	0.28	0.31	0.26	0.15
n measures on alpha-Ottawa		20	18	31	39	33	5	88	20	6	8	8
ArH_2-free plateau width (amu)		0.005	0.006 to 0.011									
Comments		*						**				***

View Article Online
DOI: 10.1039/D6JA00007J

2.6.3. Faraday cup configuration

The Faraday cup configuration followed that described by Tacail et al., 2014 [20]: C = $^{44}Ca^{+}$, L1 = $^{87}Sr^{2+}$ (m/z = 43.5), L2 = $^{43}Ca^{+}$, and L4 = $^{42}Ca^{+}$. Measurements targeted the left $^{40}ArH_2^{+}$-free plateau of the magnetic field, typically within 43.931 to 43.945 u relative to the fixed axial detector. Under the H cone configuration, Ca^{+} peak positions remained stable (i.e., ±0.001 u) during continuous multi-day operation and within ±0.005 u over 1 year. In this study, three amplifier configurations were evaluated (Table 3): a hybrid $10^{11}\Omega$ (C, L4) and $10^{13}\Omega$ (L1, L2) amplifier configuration (the main configuration of this work); a full $10^{11}\Omega$ configuration in static mode (i.e., fixed cup-amplifier pairing); and a rotating mode (i.e., where all four cups are successively paired with each of the four "rotating" amplifiers with identical integration times). When paired with a $10^{13}\Omega$ amplifier the L2 cup position was shifted of -0.0025 u compared to the $10^{11}\Omega$ configuration. Various acquisition methods and sample-standard Ca concentrations (5, 10, 20 ppm) were evaluated to identify the best compromise between practical considerations (e.g., time per measurement, Ca consumption) and analytical precision (Table 3).

Table 4: *Chromatography yields and cross-laboratory isotope measurements of reference materials in this study. 1: The bracketing sequence for alpha-Ottawa measured at the NRC and reported in this table is alpha$_{-1}$-sampleX-alpha$_0$-sampleY-alpha$_{+1}$, instead of the regular alpha$_{-1}$-sample-alpha$_{+1}$, with alpha$_{-1}$ and alpha$_{+1}$ bracketing alpha$_0$ and sample measurements, respectively (blanks omitted for concision). 2: This represents long-term 2SD values derived from the cumulated measurements of distinct analytical sessions realized over an 18-month period. 3: U propagated uncertainties were calculated using the approach described in [44] for multiple measurements, with the approximation that all replicates are part of one large sequence and without including additional uncertainty terms for multiple chromatography batches. For k=2, such U uncertainty values closely match 2SE values (down to the 4th decimal*). 4: *$\delta^{44/42}$Ca values relative to alpha-Ottawa are converted to the SRM915a scale by adding +0.500 ‰ (further described in the result section and Table S3). 5: $\delta^{44/42}$Ca values relative to alpha-WIGL are converted to the SRM915a scale by adding +0.527 ‰, following Koutamanis et al., 2021 [18]. 6: $\delta^{44/42}$Ca values relative to alpha-WIGL are converted to the SRM915a scale by adding +0.497 ‰, following the revision proposed by this study (further described in the result section and Table S3).*

		SRM 1486	SRM 1400	CACB-1	IAPSO	DOLT-5	DORM-5	TORT-3	alpha-Ottawa
Chromatography sequence type		A	A	A	B	C	C	C	D
Average Ca yields (%)		98.3	97.6	103.9	102.0	105.6	101.7	98.1	98.3
n chromatography replicates		*n* = 17	*n* = 5	*n* = 12	*n* = 3	*n* = 2	*n* = 3	*n* = 3	*n* = 2
NRC	**n measurement**	266	30	68	7	10	16	20	2458 [1]
$\delta^{44/42}$Ca (‰)	**mean (alpha-Ottawa)**	-1.00	-1.09	-0.09	0.41	-0.42	-0.33	0.29	0.00
	2 SD [2]	0.16	0.16	0.16	0.14	0.14	0.15	0.13	0.15
	U (k = 2)[3]	0.01	0.03	0.02	0.05	0.04	0.04	0.03	0.00
	mean (SRM915a)[4]	-0.50	-0.59	0.41	0.91	0.08	0.17	0.79	0.50
$\delta^{43/42}$Ca (‰)	**mean (alpha-Ottawa)**	-0.52	-0.57	-0.03	0.23	-0.27	-0.19	0.10	0.00
	2 SD [2]	0.28	0.30	0.26	0.21	0.19	0.25	0.18	0.33
WIGL	**n measurement**	7	4	5	5	6	7	5	8
$\delta^{44/42}$Ca (‰)	**mean (WIGL)**	-0.99	-1.07	-0.08	0.44	-0.31	-0.19	0.33	-0.01
	2 SD	0.22	0.1	0.14	0.19	0.1	0.36	0.2	0.18

	mean (SRM915a)[5]	-0.47	-0.54	0.45	0.96	0.22	0.34	0.86	0.52
	mean (SRM915a)[6]	-0.50	-0.57	0.42	0.93	0.19	0.31	0.83	0.49
$\delta^{43/42}$Ca (‰)	**mean (WIGL)**	-0.50	-0.56	-0.03	0.21	-0.13	-0.03	0.17	-0.02
	2 SD	0.16	0.08	0.13	0.12	0.08	0.16	0.17	0.12

2.6.4. Acquisition method

A standard-sample-standard bracketing acquisition method was used to correct the instrumental mass bias (blanks in this sequence are not shown for concision). Routine autosampler rinsing prior to each standard or sample consisted of two 5s rinses in 2 % v/v HNO_3 (TMG) followed by a 135 s take-up in a third identical blank, after which a baseline blank was collected under the same acquisition parameters as for samples and standards (Table 3). Samples and bracketing standards were analyzed after a take-up time of 90 s. For the in-house bracketing standard (alpha-Ottawa), isotopic composition relative to itself was also collected using the following sequence: alpha$_{-1}$-sampleX-alpha$_0$-sampleY-alpha$_{+1}$, where alpha$_0$ is bracketed against alpha$_{-1}$ and alpaha$_{+1}$ (blanks not shown for concision). No outlier sigma correction was applied on measured isotope ratios as it was observed to marginally worsen long-term precision in preliminary tests. Reported δCa values are primarily referenced relative to alpha-Ottawa, and secondarily to SRM915a for comparison with the literature.

The $^{87}Sr^{2+}$ beam (m/z = 43.5) was monitored to correct Sr^{2+} contributions to Ca isotopes following Tacail et al., 2014 [20]. For example for $^{43}Ca^{+}$: $V_{43\text{-}c} = V_{43} - V_{43.5} \times R_{87/86} \times (M^{86}Sr / M^{87}Sr)^f$, where $V_{43\text{-}c}$ represents the corrected signal for $^{43}Ca^{+}$, V_{43} and $V_{43.5}$ are respectively the signals of L2 and L1 cups, $R_{87/86}$ represents the certified isotopic ratio of NIST SRM987, $M^{86}Sr/M^{87}Sr$ represents the isotope mass ratios of ^{86}Sr and ^{87}Sr, and f is the mass discrimination factor. For a given isotopic ratio, $f = \ln(r^{X/Y} / R^{X/Y}) / \ln(M_X / M_Y)$, where X and Y are given isotopes, M is their atomic mass, r is the measured isotope ratio, and R the true isotope ratio (approximated from certified values). The f value was determined from the Sr^{2+} beams using a 20 ppm Sr solution of NIST SRM987 under identical instrumental conditions, yielding f values ranging from 1.3 to 1.7, approximately 0.5 lower than values measured on Ca^{+} beams. Replicated measurements not meeting requirements of matching Ca concentration, deviating significantly from the expected mass-dependent relationship (Figure 3), or obtained during transient instrumental instability were excluded from further analysis.

2.6.5. Gain calibration

Faraday amplifiers with $10^{13}\Omega$ feedback resistors provide improved signal-to-noise performance at low ion currents (5 to 200 fA). However, on Neptune Plus instruments their gain factor cannot be calibrated using the conventional constant-current method (unlike for $10^{10}\Omega$, $10^{11}\Omega$ and $10^{12}\Omega$ amplifiers). Manual gain calibration methods using various isotopic systems exist (e.g., Hf, Nd) and allow to cross calibrate $10^{13}\Omega$ amplifiers with $10^{11}\Omega$ amplifiers, offering different precision and long-term stability (see official recommendations by Thermo Fisher Scientific). For simplicity, a direct Ca-based cross-calibration was implemented using $^{43}Ca^{+}$ (L2 cup) and $^{44}Ca^{+}$ (C cup) successively measured first with $10^{11}\Omega$ amplifiers then with the $10^{13}\Omega$ amplifier assigned to the L2. The calibration solution contained 25 ppm Ca of alpha-Ottawa, yielding a $^{43}Ca^{+}$ beam of approximately 0.175 V (in $10^{11}\Omega$ equiv., 1.75 pA) in H cone configuration, within the manufacturer's recommended range of 0.1 to 0.3 V (in $10^{11}\Omega$ equiv., 1 to 3 pA). The gain factor was calculated with the following formula: gain factor = 44/43 (C: $10^{11}\Omega$, L2: $10^{13}\Omega$) ÷ 44/43 (full $10^{11}\Omega$), with each isotope ratios being measured with 100 cycle (1 block) of 16 s integration (equivalent to 27 minutes of measurement). It should be noted that the gain factors of the $10^{13}\Omega$ amplifiers to be calibrated must be manually set to 1 prior to measurements. This calibration method does not provide the best achievable precision but allows for a straightforward calibration directly on any conventional (i.e., not isotopically spiked) purified Ca solution. Since sample isotope ratios are obtained through standard-sample-standard bracketing, amplifier gain factors have little

View Article Online
DOI: 10.1039/D6JA00007J

influence on uncorrected δCa values. However, accurate cross-calibration of gain factors between the L1 cup amplifier and the rest of the used cup array is crucial for proper Sr^{2+} correction.

2.6.6. Quality assessment

Procedural Ca blank levels were monitored throughout chromatography and ICP-MS measurements. Measurement precision was evaluated through repeated analyses of the in-house standard alpha-Ottawa and all international reference materials (Table 3, Table 4). The accuracy of $\delta^{44/42}$Ca measurements was verified by comparing measured values for international reference materials against literature values and independent measurements from the WIGL. The absence of interferences and matrix-dependent biases was assessed by examining the mass-dependent relationship between $\delta^{44/42}$Ca and $\delta^{43/42}$Ca values, in accordance with the literature [20,24]. Doping experiments were conducted to evaluate the sensitivity of the analytical procedure to Fe, Mg, K, Al, and Sr contaminations, and to compare them with other analytical configurations from the literature [14,45]. Test solutions contained 10 ppm Ca of alpha-Ottawa mixed with varying concentrations of these contaminants (obtained from 1000 ppm Sigma-Aldrich single element ICP standards), resulting in X/Ca ratios ranging from 10^{-6} to 10^{-1}. Additional analyses were performed on purified SRM1486 spiked with Sr to a Sr/Ca ratio of 10^{-3}, and on unpurified CACB-1 (i.e., no chromatography) with a natural Sr/Ca ratio of approximately 4.89 x 10^{-4}.

3. Results

3.1. Chromatography procedures

Elution profiles for steps 0, 1a and 1b (Table 1) are outlined in Figure 2. Each chromatography sequence (Table 2) achieved Ca yields indistinguishable from quantitative recoveries (~100 %) within analytical precision (measured post step 2), along with effective separation of Ca from other monitored elements (Figure 2, Table 4). Each sequence also achieved Sr quantitative recovery, providing extended collection stages at steps 1a and 1b (Table 1). Seawater (IAPSO) exhibited the highest initial Sr/Ca ratio among all tested materials, at 1.92 x 10^{-2}. It showed a reduction to 1.10 x 10^{-3} after a modified step 2 (Table 1) using 100-150 µm particle size resin, indicating a 17-fold decrease. Using 50-100 µm particle size resin, the Sr/Ca ratio fell below 1.5 x 10^{-5} (the limit of detection in this study), marking a >1000-fold decrease. Similar results were observed with the other reference materials.

Cumulative procedural blanks collected throughout chromatography consistently contained below 25 ng of Ca (*n* = 12), with only three cases between 25 and 40 ng and one at 111 ng. These nano-contaminations have negligible impact on Ca isotope measurements, with samples and bracketing standards containing tens to hundreds of µg of Ca.

Ca-spiked matrix solutions produced $\delta^{44/42}$Ca values in agreement with the theoretical alpha-Ottawa value of 0‰ (0.01 ±0.03 ‰, 2SE, *n* = 35 replicates, all Ca-spiked solution pulled together). The same observation is made for Ca-spiked solutions taken individually, the δCa values of which are reported in Table S2.

3.2. Ca isotope measurements

Results from the configuration screening on the NRC's Neptune Plus are summarized in Table 3. Average $\delta^{44/42}$Ca and $\delta^{43/42}$Ca values and their respective standard deviations (SD) measured at the NRC and WIGL for reference materials are reported in Table 4. Approximately 16 % of measurement replicates were treated as outliers and excluded from further analyses based on criteria detailed in the method section, primarily due to sample-bracketing concentration mismatch. Using the default NRC configuration (see Table 3), the average 2SD of $\delta^{44/42}$Ca and $\delta^{43/42}$Ca values for all seven reference

View Article Online
DOI: 10.1039/D6JA00007J

materials are 0.15 ‰ and 0.24 ‰, respectively (n = 417), similar to alpha-Ottawa self-standardized measurements (respectively 0.15 ‰ and 0.33 ‰, 2SD, n = 2458) despite the difference of bracketing strategy.

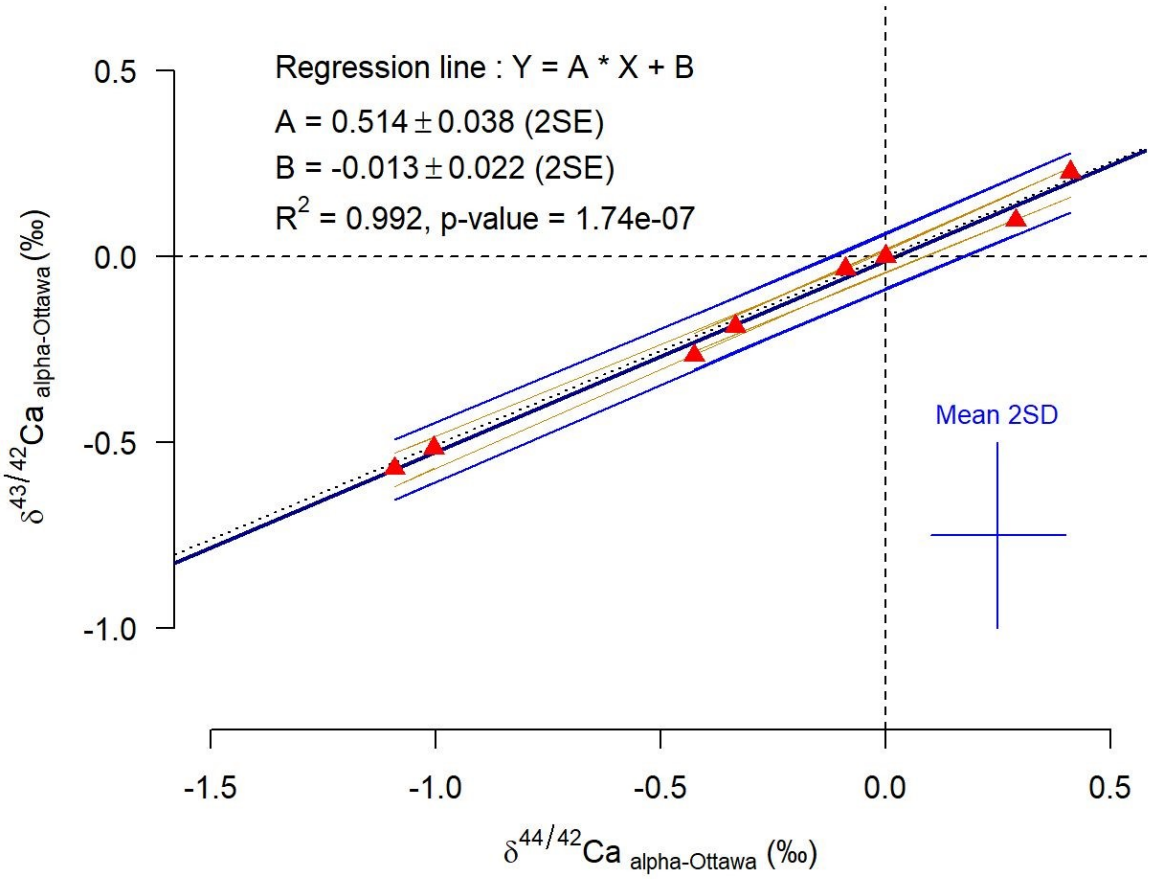

Figure 3: *Three-isotope plot of studied reference materials (red triangles, NRC values only). δCa values are expressed relative to the alpha-Ottawa primary standard. These measurements plot on a linear regression line (central dark blue solid line) with a slope of 0.514 ±0.038 (2SE) and an intercept of -0.013 ±0.022 (2SE) and are indistinguishable within uncertainties from the 0.5067 slope predicted from the exponential mass-dependent fractionation law (black dotted line). The two outer blue lines delimit the prediction interval of the regression line, while the inner orange lines show its 95 % confidence interval. This supports the assertion that no interference or instrumental bias has significantly affected the accuracy of the measurements presented in this study. The average 2SD for these $\delta^{44/42}$Ca and $\delta^{43/42}$Ca values is represented by the blue cross in the lower right of the graph (0.15 ‰ and 0.25 ‰, respectively; n = 2875).*

The δCa values of the seven reference materials independently analyzed in dry plasma configuration at the WIGL are consistent within uncertainty with NRC measurements (Table 4), supporting the accuracy of the NRC measurements and reported $\delta^{44/42}$Ca values. A compilation of $\delta^{44/42}$Ca measurements of SRM1486, SRM1400, and seawater (mostly IAPSO) from the literature and this study is provided in Table S3. The difference in $\delta^{44/42}$Ca values between IAPSO and SRM1486 measured on the NRC configuration is of 1.41 ±0.21 ‰ (2SD, n_{IAPSO} = 7, $n_{SRM1486}$ = 266). This value agrees with the results from the WIGL reported in this study (1.43 ±0.29 ‰, 2SD, n_{IAPSO} = 5, $n_{SRM1486}$ = 7) and with the literature database in Table S3 (1.41 ±0.19 ‰, 2SD, n_{IAPSO} = 836, $n_{SRM1486}$ = 1361). The conversion from alpha-Ottawa to the SRM915a δCa standard scale was derived from SRM1486 and IAPSO $\delta Ca_{alpha\text{-}Ottawa}$ values measured in this study and $\delta Ca_{SRM915a}$ literature values (reported in Table S3). SRM1400 data (also reported in Table S3) were excluded from the scale conversion formula, following evidence of inter-batch heterogeneities (Table S3). Two point-linear regressions [46] and averaged exact single-point conversions [44] produce similar results for the natural range of $\delta^{44/42}$Ca values, closely equivalent to the

addition of +0.500 ‰ when converting $\delta Ca_{alpha\text{-}Ottawa}$ to $\delta Ca_{SRM915a}$ values (Table S3). This dataset supports previous conversion formulas proposed between ICP Ca Lyon (LGL) and SRM915a primary standard scales (+0.518 ‰ in Martin et al., 2018; +0.517 ‰ in Table S3). However, it also supports a minor revaluation of the formula for converting WIGL data to SRM915a primary standard scale (+0.497 ‰ see Table S3; previously estimated at +0.527 ‰, Koutamanis et al., 2021). It can be noted that despite minor differences, all three above-mentioned Thermo Fisher Scientific-based Ca solutions (previously Alpha Aesar) used as bracketing standards and in-house primary standard (ICP Ca Lyon, WIGL, alpha-Ottawa) stay within uncertainties from each other, especially between alpha-Ottawa and WIGL. This is shown in Table 4 original data (alpha-Ottawa measured against WIGL: -0.01 ±0.18 ‰, 2SD) and Table S3 literature data ($\delta^{44/42}Ca_{alpha\text{-}Ottawa} \approx \delta^{44/42}Ca_{ICP\ Ca\ Lyon} + 0.014$ ‰, $\delta^{44/42}Ca_{alpha\text{-}Ottawa} \approx \delta^{44/42}Ca_{WIGL} - 0.003$ ‰).

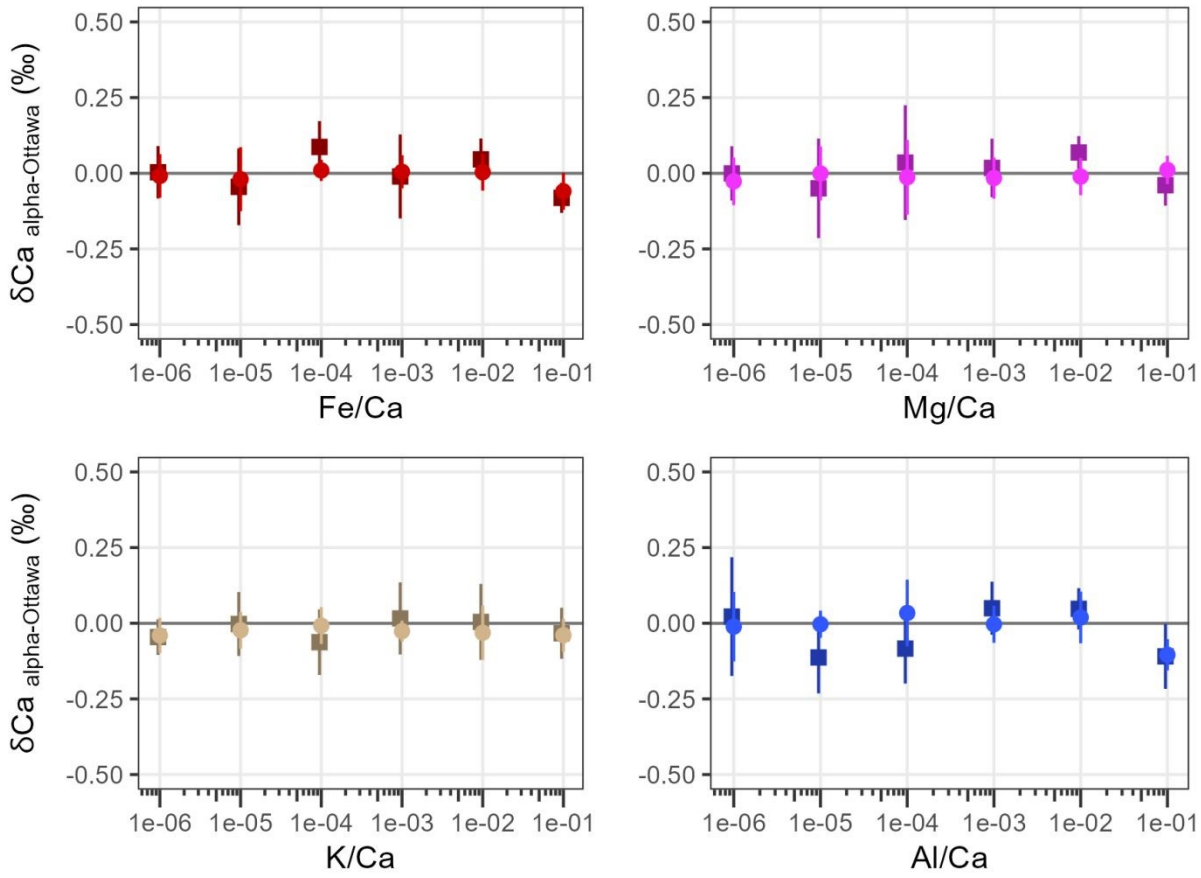

Figure 4: *Fe, Mg, K and Al doping effects on $\delta^{44/42}Ca$ values (circles) and $\delta^{43/42}Ca$ values (squares) of alpha-Ottawa (10 ppm of Ca). Error bars are given as ±2 standard error of the mean (2SE). Each reported δCa value is the mean of n = 3 to 9 replicated measurements. The data used to make these figures are detailed in Table S4. Tested concentrations of listed contaminants have limited effect on measured $\delta^{44/42}Ca$ and $\delta^{43/42}Ca$ values. Only a minor negative shift is tentatively observed for Fe/Ca and Al/Ca = 10^{-1}, but at the limit of what instrumental precision allows to reliably identify.*

After conversion to the same referential, SRM1400 and TORT-3 $\delta^{44/42}Ca$ values measured in this study (Table 4) are in agreement with literature values reported in Table S3 (omitting two SRM1400 flagged as outliers in the table) and Delette et al., (2025) for TORT-3, further supporting the reliability and accuracy of the proposed chromatography and analytical procedures.

The mass dependent relationship between $\delta^{44/42}Ca$ and $\delta^{43/42}Ca$ values is shown in Figure 3. The linear regression line yields a slope in agreement with the theoretical slope of 0.5067 predicted by the exponential mass-dependent fractionation law, supporting the absence of significant interferences or uncorrected instrumental bias affecting δCa values.

View Article Online
DOI: 10.1039/D6JA00007J

The results of doping experiments are presented in figure 4 for Fe, Mg, K, Al and in figure 5 for Sr (respective data are detailed in Table S4 and Table S5). Figure 4 shows that additions of Fe, Mg, K, or Al up to a X/Ca ratio of 10^{-2} produce no detectable effect on $\delta^{44/42}Ca$ and $\delta^{43/42}Ca$ values, with only a possible onset of negative shifts at Fe/Ca and Al/Ca of 10^{-1} (at the limit of instrumental precision). Figure 5 highlights that without Sr correction, $\delta^{44/42}Ca$ and $\delta^{43/42}Ca$ values deviate significantly from the expected 0‰ at a Sr/Ca ratio above 10^{-5}, consistent with observations on other ICP-MS configurations [8,24,26,37]. Applying Sr^{2+} correction restores accurate $\delta^{44/42}Ca$ and $\delta^{43/42}Ca$ values up to Sr/Ca ratios of 10^{-3} with proper gain calibration (Figure 5a and c), potentially extending to 10^{-2} using precise gain calibration with the hybrid 10^{11}-10^{13} amplifier configuration detailed previously (Figure 5c). The accuracy of this correction is further supported by the post-chromatography SRM1486 solution spiked to a Sr/Ca ratio of 10^{-3}, which yielded a $\delta^{44/42}Ca$ value of -0.97 ±0.03 ‰ (2SE, n = 4), in agreement with its Sr-free equivalent. Similarly, an unpurified CACB-1 solution (without chromatography), with a Sr/Ca ratio of about 4.89 x 10^{-4}, yielded a $\delta^{44/42}Ca$ value of -0.06 ±0.08 ‰ (2SE, n = 9), which is consistent with its post-chromatography counterpart.

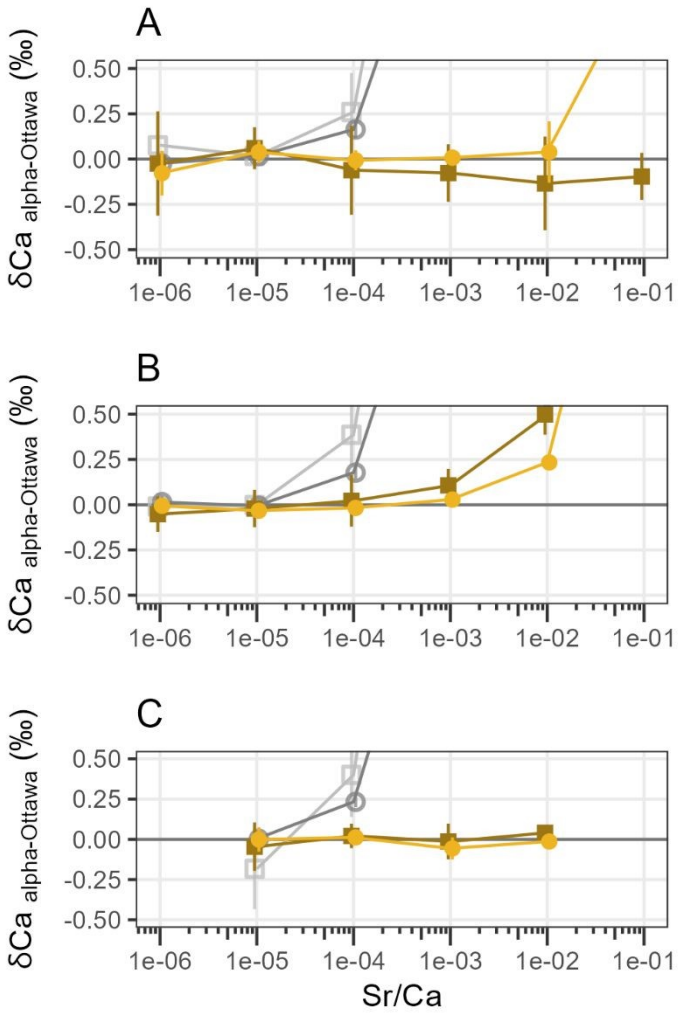

Figure 5: *Sr doping effects on $\delta^{44/42}Ca$ and $\delta^{43/42}Ca$ values of alpha-Ottawa (10 ppm of Ca), with (A) a full 10^{11} rotating amplifier configuration, (B) a hybrid 10^{11}-10^{13} amplifier configuration with 10^{13} amplifiers on mass 43 and 43.5 but with outdated gain calibration (> 6 months) and (C) with gain calibration dating from the previous day. Grey open marks and yellow closed marks respectively represent uncorrected base measurements and Sr^{2+} corrected values, with circles and squares representing $\delta^{44/42}Ca$ and $\delta^{43/42}Ca$ values, respectively. Error bars are given as ±2 standard error of the mean (2S,). Each reported δCa value is the mean of n = 2 to 7 replicated measurements. The data used to make these figures are detailed in Table S5. The hybrid amplifier configuration (B, C) can allow to reliably correct Sr^{2+} interferences up to a Sr/Ca of 10^{-2} providing up-to-date gain calibration and mass discrimination factor (f) quantification (C only).*

View Article Online
DOI: 10.1039/D6JA00007J

4. Discussion

4.1. Chromatography developments

4.1.1. General design

The negligible Ca procedural blanks (typically < 25 ng), quantitative Ca recovery (Table 4), and efficient Ca separation from matrix elements (Figure 2) across all tested materials and chromatography sequences demonstrate that the proposed branching chromatography procedure meets the key prerequisites for accurate Ca isotope measurements. Ca-spiked matrix solutions displayed no deviation from the alpha-Ottawa Ca isotopic composition (0.01 ± 0.03 ‰, 2SE, *n* = 35 replicates, Table S2), confirming the absence of significant isotopic fractionation of Ca isotopes during chromatography. For Sr isotope applications, Sr quantitative recovery from the same aliquot was also possible, providing an extension of the collection stages of steps 1a and 1b (Table 1).

By adapting existing procedures [20–22,36], the tailored chromatography sequences developed in this study accommodate sample-specific matrices (Table 1, Table 2), providing a versatile approach while optimizing time, minimizing reagent usage, and favoring widely accessible labware. Compared to other analogous procedures (e.g., [20,21]), the loading volume of step 0 (3.5 ml, Table 1) is relatively large for the volume of resin (2 ml of AG® 1-X8), logically leading to peak widening. This unconventional large loading volume was required to process large amounts of low Ca/matrix material (equivalent to a maximum of 91 mg of material pre-digestion for DOLT-5) necessary to yield sufficient Ca (> 20 µg). Importantly, this adjustment did not compromise Fe, Cu, and Zn separation from the Ca fraction (Figure 2). Another specificity is the use of Eichrom Sr resin with 50-100 µm particle size, instead of the 100-150 µm particle size more commonly employed (e.g., [20,22]). The implications of this choice are discussed in the following section.

4.1.2. Matrix purification and tolerance

Although the medium resolution slit mode of the MC-ICP-MS resolves some interferences, molecular products of Mg, K, and Al can still interfere with $^{42}Ca^{+}$, $^{43}Ca^{+}$ and $^{44}Ca^{+}$ signals when too abundant [2]. Moreover, Fe can indirectly interfere with Ca isotope measurements by inducing matrix effects, i.e., by altering relative ion transmission when Fe concentrations exceed certain thresholds [20,45,48,49]. Doping experiments show that, across most of the tested 10^{-6} to 10^{-1} range of X/Ca ratios (where X is Fe, Mg, K, or Al), $\delta^{44/42}Ca$ and $\delta^{43/42}Ca$ values are not significantly affected, with only marginal shifts possibly detected for Fe/Ca and Al/Ca of 10^{-1} (Figure 4). These thresholds largely exceed typical post-chromatography ratios, confirming that reported Ca isotope measurements are unaffected by such interferences. Nevertheless, these results provide a complementary guide for selecting appropriate chromatography sequences (Table 2) for different materials. It should be noted, however, that these thresholds were established using relatively pure 2 % HNO_3 solutions containing only Ca and one signal dopant element per solution, and cannot be directly extrapolated to more complex cases with multiple co-occurring contaminants.

Results from this study (wet plasma, H cone configuration, [Ca] = 10 ppm) are similar to those of Bao et al., 2020 (wet plasma, jet & X cone configuration, [Ca] = 5 ppm), albeit without the tentatively observed marginal deviation at X/Ca = 10^{-1} for Fe and Al (Figure 4). However, both this study and Bao et al., 2020 differ from results reported by Hassler, 2021 on the same instrument but with distinct configuration (dry plasma, jet & X cone configuration, [Ca] = 1.25 ppm), where $\delta^{44/42}Ca$ and $\delta^{43/42}Ca$ deviations tend to start at lower X/Ca thresholds (often around X/Ca = 2.10^{-2}) and to be of greater amplitude, most notably for Fe. Although these three studies do not share the exact same list of tested elements, X/Ca range and resolution, these comparisons suggest that wet plasma configurations (e.g.,

[14] and this study) exhibit greater tolerance to certain matrix effects than dry plasma configurations working at lower Ca concentrations (e.g., [20,45]). These findings reaffirm that contamination thresholds and deviation magnitudes are configuration-specific and should be treated accordingly.

4.1.3. Advances in Sr removal for Ca purification

Despite switching to a smaller particle Sr resin (50-100 µm instead of 100-150 µm) and making minor adjustments to elution volumes, step 2 of the chromatography (Table 1) achieved results comparable to Guiserix et al., 2022 [22]. However, the smaller particle size resin achieved enhanced Ca-Sr separation, producing Sr/Ca ratios in the Ca fraction near detection limits for all tested materials (Sr/Ca < 1.5 x 10^{-5}, [Sr] < 150 ppt). This high degree of purification enables the analysis of high Sr/Ca samples, such as seawater (1.92 x 10^{-2}) and soft tissues (4.91 x 10^{-3} to 1.39 x 10^{-2}), without requiring Sr^{2+} signal correction (Figure 5). Comparatively, the same procedure applied with 100-150 µm particle size resin only reduced the Sr/Ca ratio of IAPSO to 1.10 x 10^{-3} (a 17-fold reduction, instead of >1000-fold), requiring Sr^{2+} signal correction (Figure 5). However, finer resin results in a slower flow rate, extending this chromatography step to a full working day, compared to the ⅔ to ½ day with the larger particle size resin.

Both resin grades have similar capacity factors, exceeding the highest Sr loads (1 µg of Sr) of the analytes in this study by about 600 to 4000 times [50,51], so performance differences are not capacity-driven. The finer Sr-resin offers better separation power, with narrower elution curves and reduced peak fronting [50]. Peak fronting may explain why some Sr co-elutes with the Ca fraction using the 100-150 µm grade resin. Although 3.5 ml of 3M HNO_3 loaded during the Ca collection phase is a relatively small volume regarding the theoretical free column volume [50], mechanical properties of the resin grades may contribute to their differences in performance. Resin beds prepared with the 50-100 µm grade (mixed with ultrapure water) form more cohesive packings when deposited by gravity into columns, whereas 100-150 µm particles are prone to form micro-porosities near column walls, potentially coalescing into micro-channels in the most severe cases, causing earlier peak fronting. Such porosities are difficult to detect and correct, even with overnight resin-water mixing and repeated refluxing during the preparation of resin bed by gravitational deposition (see Supplementary information). Future studies could test whether pressure-packing 100-150 µm resin (e.g., in-house with N2 gas [52], or a commercial equivalent) can improve Ca-Sr separation to more satisfactory levels with shorter elution times. Using columns with better aspect ratios may also help mitigate these shortcomings (albeit with potentially longer elution times), though preliminary tests that included larger resin volumes with identical column shapes showed limited success in this regard (see Supplementary information). Alternatively, Sr^{2+} interference correction can compensate for those issues during Ca isotope analyses (further discussed in the following sections).

Reusing Eichrom Sr resin for multiple elutions can be problematic due to Sr carryover after conventional washes with highly diluted HNO_3 (< 0.5 M) or ultrapure water [53,54], while using fresh resin for each sample incurs high costs. Although not tested here, prior studies suggest that thorough rinsing with HCl or chelating agents (e.g., [55,56]) may enable resin reuse and reduce costs. For Ca isotope applications specifically—where Sr is not collected—resin reuse could prove more feasible, since Sr affinity for the resin is high during Ca elution.

4.2. Benefits of $10^{13}\Omega$ amplifiers

4.2.1. Accuracy and precision in a low transmission configuration

Operating in a low ionic transmission configuration poses challenges for measuring the $^{43}Ca^{+}$ signal (the least abundant of the ^{44}Ca, ^{43}Ca and ^{42}Ca isotope trio) and obtaining precise $\delta^{43/42}Ca$ values when relying on conventional $10^{11}\Omega$ amplifiers (see Table 3 2SD values). Beam intensities below 1 pA (equivalent to 0.1 V on a $10^{11}\Omega$ amplifier), as with $^{43}Ca^{+}$ when employing the default configuration of

View Article Online
DOI: 10.1039/D6JA00007J

this work (0.6 to 0.9 pA, Table 3), approach the lower operational limits recommended for this amplifier class, leading to relatively low signal/noise ratios and high $\delta^{43/42}$Ca 2SD values (Table 3, [31]). Utilizing a $10^{13}\Omega$ amplifier for $^{43}Ca^{+}$ improved performance by yielding a $\delta^{43/42}$Ca 2SD value of 0.21 ‰ (n = 88) during preliminary tests on alpha-Ottawa (Table 3), and a long-term average 2SD value of 0.25 ‰ across secondary standards (Table 4). Although this 2SD is about twice that typically reported in the MC-ICP-MS literature (see references in Table S3), it represents a twofold improvement over the 0.42 ‰ (2SD, n = 18) otherwise obtained under the same conditions with $10^{11}\Omega$ amplifiers (Table 3). This level of precision for $\delta^{43/42}$Ca measurements meets routine quality control requirements, typically requiring 3-4 replicates per sample for reliable mass dependency assessment (Figure 3), similar to what is preferable for the accurate determination of $\delta^{44/42}$Ca values. For $\delta^{44/42}$Ca measurements, the most central metric for Ca stable isotope applications in absence of a measurable $^{40}Ca^{+}$ signal, both ^{44}Ca and ^{42}Ca signals were measured using conventional $10^{11}\Omega$ amplifiers throughout this work and delivered satisfactory 2SD values, consistent with literature standards (2SD = 0.12 ‰, Table 3; 2SD = 0.15 ‰, Table 4; see Table S3 for comparison). As previously detailed in the result section, reference material data produced using the default configuration (Table 3) agree with values from the literature (Table S3, Delette et al., 2025 [27]), as well as with independent measurements from the WIGL (Table 4), jointly supporting the measurement accuracy of this method. These observations support that measuring Ca isotopic compositions with good levels of accuracy, precision and quality control is possible for low transmission configurations when coupled with the proposed amplifier configuration.

Future tests could explore whether increasing sample and bracketing standard Ca concentrations above 10 ppm could improve precision without causing issues (e.g., cone clogging), as suggested by preliminary tests at 20 ppm (Table 3). However, this would necessitate more destructive sampling to meet Ca instrumental demands. Furthermore, in this study no tests were made on $10^{12}\Omega$ amplifiers. However, $^{43}Ca^{+}$ signal intensities measured in the default setup of this work (Table 3) fall well within the operational range of $10^{12}\Omega$ amplifiers. As Neptune Plus ICP-MS instruments allow simpler calibration routine for $10^{12}\Omega$ amplifiers (constant current method), they could represent a promising alternative, potentially offering improved precision while simplifying analytical workflows.

4.2.2. Minimum sampling requirements

While the default configuration detailed here achieves satisfactory precision for $\delta^{43/42}$Ca values, it also reveals a reduction in precision compared to the literature (Table 3 versus Table S3). By default, $^{43}Ca^{+}$ beam intensities were maintained in the upper range of $10^{13}\Omega$ amplifiers' capacity (around 0.4 pA on average). Lowering $^{44}Ca^{+}$ and $^{42}Ca^{+}$ beam intensities to match the levels tested for $^{43}Ca^{+}$ (to reduce Ca analytical requirements for example) would likely produce $\delta^{44/42}$Ca 2SD values similar to those reported for $\delta^{43/42}$Ca. This would limit many applications from the literature, as most require low $\delta^{44/42}$Ca 2SD values, unlike for $\delta^{43/42}$Ca used for the sole purpose of quality control here. Therefore, maintaining $^{42}Ca^{+}$ beam (and the more abundant $^{44}Ca^{+}$) in a higher range of intensity, above 1 pA, seems preferable. Further decreasing $^{43}Ca^{+}$ beam intensities could also hamper the usage of lower sample-standard Ca concentrations by limiting quality control capabilities through progressively worsening $\delta^{43/42}$Ca 2SD values. According to manufacturer documentation and the literature, $10^{13}\Omega$ amplifiers are reliable down to 5 fA, but with measurement precision which nonetheless degrades with decreasing ion beam intensity (explored in Table 3 and [31]). This shows that further decreasing Ca ion beam intensities has some limits, and that the use of $10^{13}\Omega$ amplifiers in low ionic transmission configuration do not allow to decrease Ca consumption lower than higher transmission configurations using $10^{11}\Omega$ amplifiers. However, results suggest that combining this amplifier configuration within higher ionic transmission (e.g., dry plasma and/or large aperture cone configurations) could divide Ca analytical requirements by factors of 5 to 30 (typically below 1 µg of Ca for triplicate measurements) compared to conventional solution MC-ICP-MS procedures of the literature (providing equal precision per ion beam intensities), as previously envisioned [7]. Such improvements would particularly benefit studies of precious geo-, bio-, paleo- and archaeo-archives, where minimizing sampling requirements is critical due to the

View Article Online
DOI: 10.1039/D6JA00007J

frequently finite nature of source samples. They could also enhance the maximum spatial sampling resolution for conventional/mechanical sampling techniques (e.g., enamel or dentine serial micro-drilling) and facilitate studies of Ca-poor matrices (e.g., insect body parts).

4.2.3. Sr^{2+} correction with improved detectors

Ca isotope measurements by MC-ICP-MS are highly sensitive to Sr^{2+} interferences, with significant biases arising even with only nanograms of Sr (i.e., for Sr/Ca > 10^{-5}, see uncorrected signal in Figure 5). The $^{87}Sr^{2+}$ signal intensity, used to correct $^{44}Ca^{+}$, $^{43}Ca^{+}$ and $^{42}Ca^{+}$ from other doubly charged Sr isotopes ($^{88}Sr^{2+}$, $^{86}Sr^{2+}$, $^{84}Sr^{2+}$), is typically low (e.g., 0.2 pA/ppm or 0.02 V/ppm in $10^{11}\Omega$ equivalent with this study's default setup). When using only $10^{11}\Omega$ amplifiers in rotating mode (Figure 5a), the accuracy and precision of corrected $\delta^{44/42}Ca$ and $\delta^{43/42}Ca$ values deteriorate beyond Sr/Ca ratios of 10^{-2} and 10^{-3}, respectively. This degradation appears earlier for $\delta^{43/42}Ca$ (Figure 5a), in part because a $10^{11}\Omega$ amplifier was used for $^{43}Ca^{+}$ in this test. Employing a $10^{13}\Omega$ amplifier for $^{87}Sr^{2+}$ (and $^{43}Ca^{+}$) with updated gain calibration (Figure 5c) preserves accurate and precise $\delta^{44/42}Ca$ and $\delta^{43/42}Ca$ values across the entire tested range, up to Sr/Ca ratios of 10^{-2}. This represents a significant improvement over earlier studies, where Sr^{2+} corrections often fail beyond Sr/Ca ratios of 2x 10^{-4} (e.g., [26]) or 5 x 10^{-3} (e.g.,[37]). This enhanced tolerance to Sr contamination expands the range of analyzable samples without extensive Sr removal by chromatography or Sr correction by standard addition [38]. The robustness of this Sr^{2+} correction method is further supported by results from the non-purified CACB-1 solution (Sr/Ca = 4.89 x 10^{-4}) and the Sr-spiked post-chromatography SRM1486 solution (Sr/Ca = 10^{-3}), as both solutions yielded $\delta^{44/42}Ca$ values consistent with their Sr-free equivalents (Table 4 versus Table S5).

While the standard-sample-standard bracketing method eliminates the need for precise amplifier gain calibration for δCa isotope ratio measurements, Sr^{2+} correction reintroduces this dependency (see method section). Consequently, the quality of Sr^{2+}-corrected δCa values relies on both accurate amplifier gain calibration and the stability of instrumental mass bias (Figure 5b versus Figure 5c). For Neptune plus MC-ICP-MS instruments, $10^{13}\Omega$ amplifier gain calibration must be performed manually. The enhanced Ca-based approach presented here (see method section) integrates into the initial tuning phase of a week-long analytical session without requiring repeated calibrations (alternative calibration methods using other elements may offer accuracy and precision benefits; e.g., [57]). However, high Sr/Ca ratios (> 10^{-3}) increase dependence on gain calibration accuracy, potentially necessitating more frequent calibrations to maintain the accuracy of Sr^{2+}-corrected δCa values. Using $10^{13}\Omega$ constant current gain calibrations (possible with newer MC-ICP-MS models) could streamline this workflow. Another potential strategy is using $10^{12}\Omega$ amplifiers (not tested here), which benefit from routine constant-current gain calibration on Neptune Plus instruments and could improve Sr^{2+} correction performance. However, this approach may not suit low ionic transmission configurations, as $^{87}Sr^{2+}$ beam intensity remains extremely low (<0.03 pA for Sr/Ca = 10^{-2}), challenging the operational limits of this amplifier class.

When precise gain calibration is critical, signal acquisition using amplifiers in rotating mode (where amplifiers are successively paired with every Faraday cup in use) can reduce gain calibration errors (e.g., [58]). This notably explains how a full $10^{11}\Omega$ amplifier configuration could maintain stable accuracy and precision of $\delta^{44/42}Ca$ values across an extended Sr/Ca range, even at low ion beam intensities (Figure 5a). By contrast, $10^{13}\Omega$ amplifiers cannot operate in rotating mode on Neptune plus instruments due to software-locks designed to prevent accidental exposure to high-intensity beams. Hypothetically, employing four $10^{12}\Omega$ amplifiers could handle the wide range of ion beam intensities of $^{44}Ca^{+}$, $^{43}Ca^{+}$, $^{42}Ca^{+}$ and $^{87}Sr^{2+}$ (for high Sr/Ca), while allowing amplifier rotation and maintaining good signal-to-noise ratios. However, maintaining all beam intensities in the right range would be challenging (e.g., risks of unintended exposure to high-intensity ion beams), and with benefits that remain to be quantified.

At relatively high Sr/Ca ratios, the stability of the mass discrimination factor *f* is also crucial for accurate and precise Sr^{2+}-corrected δCa values. In this study, *f* was determined using the Sr^{2+} ion beams from a 20 ppm Sr solution of SRM987 (NIST). Occasional measurements of *f* were performed prior to Ca analytical sessions involving high Sr/Ca ratios, using the same instrumental settings as for Ca isotope analyses. For consistently high Sr/Ca ratios, more frequent *f* measurements tailored to expected Sr/Ca ratios and instrument stability are advisable. In such cases, inserting Sr-spiked Ca bracketing standard solutions as secondary standards within the analytical sequence would help monitor Sr^{2+} correction quality, alongside tracking the relationship between $\delta^{43/42}Ca$ and $\delta^{44/42}Ca$ values (Figure 3). Configurations designed to improve instrumental mass bias stability for Ca^{+} and Sr^{2+} signals, analogous to approaches documented for Nd isotopes [49], could further minimize short-term variations in *f* and improve the reliability of Sr^{2+} corrections.

The conversion from the $^{87}Sr^{2+}$ signal to correct $^{84}Sr^{2+}$, $^{86}Sr^{2+}$ and $^{88}Sr^{2+}$ interferences in Ca isotope measurements relies on the certified Sr isotope ratios of NIST SRM987 (see method section). However, because ^{87}Sr is radiogenic, its relative abundance varies widely in natural materials (see Spies et al., 2025 for a review [59]). Thus, measured δCa values for samples with both high Sr content and Sr isotope ratios significantly different from SRM987 may be inaccurately corrected using this method, in which case the use of alternative reference material with certified Sr isotope ratios matching those of the samples would be advised. Caution is therefore advised for Sr^{2+} corrections in high Sr/Ca contexts, although deviations in sample $\delta^{43/42}Ca$ and $\delta^{44/43}Ca$ values from the expected mass-dependent fractionation law (Figure 3) would be a clear marker in case of non-matching Sr isotopic compositions.

4.3. International reference materials and δCa primary standard

Further detailed in the result section, the default instrumental configuration used in this study yielded $\delta^{44/42}Ca$ results consistent with measurements from the WIGL (Table 4) and the literature (Table S3). Tested reference materials cover a $\delta^{44/42}Ca$ range of –1.09 to 0.41 ‰ relative to alpha-Ottawa (Table 4), encompassing a large portion of natural Earth Ca isotopic compositions (typically -2 to 0.5 ‰, converted from Gussone et al., 2016 [2] and Tacail et al., 2020 [6]) and convenient for monitoring Ca isotope mass dependency (Figure 3). The $\delta^{44/42}Ca$ values from newly analyzed (CACB-1, DOLT-5, DORM-5, TORT-3) [39–42] and more established (SRM1400, SRM1486, IAPSO) reference materials expand the Ca isotope toolkit, supporting method validation and inter-laboratory comparability, especially as the Ca isotope community lacks a consensus commercially available primary standard for expressing δCa values.

Historically, next to seawater, the Ca carbonate SRM915a (NIST) has been widely used as δCa primary standard in literature, though it has been out of stock since 2006 [2,34]. Its successor, SRM915b, featured in numerous works (e.g., [13,60–65]), is also out of stock, while the last iteration, SRM915c, has seen little use by the Ca isotope community to this date. These Ca carbonates require minimal to no chromatography and/or Sr^{2+} signal correction, explaining their widespread use as primary standards. The newly analyzed CACB-1 from NRC shares these properties, positioning it as a potential alternative of Ca isotope primary standard. NRC materials exhibit high homogeneity, though multi-batch Ca isotope analyses for CACB-1 are needed to formally confirm δCa homogeneity across units, as all analyses reported here were from a single bottle. CACB-1 is more ^{44}Ca-enriched compared to NIST Ca carbonates, offering a distinct δCa reference. Singularly, CACB-1 Ca isotopic composition is close to the Thermo Fisher Scientific-based Ca solutions (previously Alpha Aesar) used as bracketing standards in several laboratories worldwide, including University of Ottawa and NRC (CACB-1 relative to alpha-Ottawa: $\delta^{44/42}Ca$ = -0.09 ±0.16 ‰, 2SD, *n* = 68), WIGL (CACB-1 relative to alpha-WIGL: $\delta^{44/42}Ca$ = -0.08 ±0.14 ‰, 2SD, *n* = 5) and LGL (see inter-standard comparisons, Table S3), although reported non-homogeneity between batches of this type of solutions suggests this may be coincidental [19].

View Article Online
DOI: 10.1039/D6JA00007J

As previously mentioned, seawater is also widely used in literature (Table S3). Despite requiring more extensive chromatography than the aforementioned carbonates, the consistent global ocean Ca isotopic composition (within analytical precision) and its accessibility as an in-house or international reference material (e.g., IAPSO from OSIL) make it a prime standard since the early days of Ca stable isotope geochemistry [1,4,66,67]. Additionally, seawater is among the most ^{44}Ca-enriched common material (Table 4), a useful attribute for exploring Ca mass-dependent isotopic fractionation when paired with more ^{44}Ca-depleted materials (Figure 3).

Steamed bone SRM1486 (NIST) has seen increasing use as a secondary standard, paralleling Ca isotope application development in bioapatite (see Table S3 and reference therein). Like seawater, it requires chromatographic purification before Ca isotope analysis (excluding in-situ laser ablation). Its relatively ^{44}Ca-depleted composition (Table 4) makes it useful for monitoring Ca isotopic mass dependency in tandem with more ^{44}Ca-enriched materials (e.g., IAPSO seawater, CACB-1, TORT-3). The ashed bone SRM1400 (NIST) shares similar properties and usage, though a review of the literature suggests potential inter-batch heterogeneities requiring further investigation (Table S3).

Newly analyzed soft tissue reference materials—DOLT-5 (dogfish liver), DORM-5 (fish protein) and TORT-3 (lobster hepatopancreas)—provide good secondary standards for soft tissue and marine biology applications, especially for studying samples of similar matrices (low Ca/matrix ratio). While processing these materials is more challenging (notably DOLT-5, requiring thorough acid digestion and Type C chromatography, Table 2), effective Ca purification and precise analysis were achieved (see previous sections and Table 4). Together, they span a moderately large $\delta^{44/42}$Ca range of 0.71 ‰ (Table 4), suitable for method validation and inter-laboratory comparison. A recent independent publication regarding TORT-3 Ca isotope composition further supports its inter-batch isotopic homogeneity [27].

5. Conclusion

This study resolves several issues which currently limit Ca-isotope applications and enhance the more widespread useability of the technique. Here, a branching chromatography protocol built from readily-available labware is presented, an approach that yields clean Ca and Sr fractions from a range of different substrates including carbonates, bioapatite, seawater, and soft tissues. Gravity-loaded columns with 50–100 µm particle size Sr resin drastically improves Sr-Ca separation compared to coarser resin grades, achieving ppt-levels of Sr in the Ca fraction and effectively suppressing doubly charged Sr (Sr^{2+}) interference, even without dedicated signal correction. Under wet-plasma MC-ICP-MS conditions, deploying a 10^{13} Ω Faraday cup amplifier for the $^{43}Ca^{+}$ beam enables accurate and precise $\delta^{43/42}$Ca measurements, even in low ionic transmission, and supports robust mass dependency quality control. This broadens the applicability of Ca isotope analyses to more analytical setups and laboratories, while also supporting the future deployment of configurations requiring less destructive sampling. This class of amplifier also improves Sr^{2+} corrections, maintaining accuracy and precision across a range of Sr/Ca ratio up to 10^{-2} and therefore limiting the need for Sr-dedicated chromatography, provided that amplifier gain calibration and mass-bias are rigorously controlled. Finally, this study expands the range of reference materials with different matrices relevant to other studies by reporting high-precision δCa values for seven international standards, including newly characterized CACB-1 (carbonate) and marine soft tissues (DOLT-5, DORM-5, TORT-3). Here, CACB-1 is identified as a promising successor (or complement) to the discontinued NIST SRM915a and 915b CRMs. Together, these advances serve to lift analytical barriers and strengthen inter-laboratory comparability, enabling broader, high-confidence use of Ca isotopes, notably in paleoenvironmental reconstruction, ecological trophic tracing, and biomedical research.

View Article Online
DOI: 10.1039/D6JA00007J

Author contributions

Sample preparation: A.H., E.L.; Column chromatography: A.H., E.L.; Elemental analyses: A.H., E.L.; Isotopic analyses: A.H., L.Y., A.D., F.D.; Funding acquisition: A.H., C.B., K.B.; Study design: A.H., with input from L.Y., Z.M., C.B., K.B.; Supervision: A.H., C.B., K.B.; Writing – original draft: A.H.; Writing – review & editing: all coauthors. Senior authors Kate Britton and Clement P. Bataille contributed equally.

Conflicts of interest

There are no conflicts to declare.

Data availability

The data supporting this article have been included as part of the Supplementary Information.

Fundings and acknowledgements

This work was supported by the UKRI Postdoc guarantee fund (EP/X023249/1) of the MSCA-selected project PleistoDem (call 2021), as well as NSERC Discovery Grant RGPIN-2019-05709 and New Frontiers in Research Fund Exploration NFRFE-2023-00365.

During the writing of this work, the authors used Le Chat (Mistral AI) for the purpose of rewording and rephrasing parts of the original manuscript written by the authors, and by explicitly precluding the generation of new axes of discussions or modifications of references to the literature. After this tool was used, all authors reviewed and edited the manuscript and take full responsibility for the content of the publication.

We are grateful to Jonathan O'Neil for granting us access to his clean lab facility, as well as Victor Botelho Perez Garcia, Daniel Stepner and the rest of his team for diligently sharing this space with us. We thank Hanika Rizo Garza and her team for sharing Sr resin experience and reference materials. We are grateful to Smitarani Mohanty and Nimal De Silva for their assistance regarding elemental analyses. We thank Michelle Chartrand for her tangible and intangible support to this project. Beyond the co-authors of this work and above-named persons, we extend our sincere gratitude to all the remainder members of the SAiVE team and Department of Earth and Environmental Sciences of the University of Ottawa, the NRC Metrology Research Centre of Ottawa, and Department of Archaeology of the University of Aberdeen, for fostering inclusive, supportive and collaborative research environments.

References

1 W. A. Russell, D. A. Papanastassiou and T. A. Tombrello, *Geochim. Cosmochim. Acta*, 1978, **42**, 1075–1090.

2 N. Gussone, E. Tipper, A. Schmitt, H. Alexander, W. Frank, D. Martin and M. Schiller, *Calcium Stable Isotope Geochemistry*, Springer-Verlag Berlin Heidelberg, 2016.

3 J. Skulan and D. J. DePaolo, *Proc. Natl. Acad. Sci. U. S. A.*, 1999, **96**, 13709–13713.

4 J. Skulan, D. J. DePaolo and T. L. Owens, *Geochim. Cosmochim. Acta*, 1997, **61**, 2505–2510.

5 J. E. Martin and K. Jaouen, *Annu. Rev. Earth Planet. Sci.*, 2025, **53**, 119–140.

6 T. Tacail, S. Le Houedec and J. L. Skulan, *Chem. Geol.*, 2020, **537**, 119471.

7 R. Chakrabarti, S. Mondal, A. D. Jacobson, M. Mills, S. J. Romaniello and H. Vollstaedt, *Chem. Geol.*, 2021, **581**, 120398.

8 F. Lanping, L. Zhou, L. Yang, W. Zhang, Q. Wang, T. Shuoyun and Z. Hu, *J. Anal. At. Spectrom.*, 2018, **33**, 413–421.

9 S. J. Romaniello, M. P. Field, H. B. Smith, G. W. Gordon, M. H. Kim and A. D. Anbar, *J. Anal. At. Spectrom.*, 2015, **30**, 1906–1912.

10 K. Harouaka, M. Mansor, J. L. Macalady and M. S. Fantle, *Geochim. Cosmochim. Acta*, 2016, **184**, 114–131.

11 A. Retzmann, D. Walls, K. Miller, M. Wieser, J. Irrgeher and T. Prohaska, *Monatshefte für Chemie - Chemical Monthly*, 2021, **152**, 401–410.

12 W. Dai, F. Moynier, M. Cui and J. Siebert, *Journal of Trace Elements and Minerals*, 2023, 100082.

13 W. Dai, F. Moynier, M. Paquet, J. Moureau, B. Debret, J. Siebert, Y. Gerard and Y. Zhao, *Chem. Geol.*, 2022, **590**, 120688.

14 Z. Bao, C. Zong, K. Chen, N. Lv and H. Yuan, *Int. J. Mass Spectrom.*, 2020, **448**, 116268.

15 R. Grigoryan, M. Costas-Rodríguez, R. E. Vandenbroucke and F. Vanhaecke, *Anal. Chim. Acta*, 2020, **1130**, 137–145.

16 M. Li, Y. Lei, L. Feng, Z. Wang, N. S. Belshaw, Z. Hu, Y. Liu, L. Zhou, H. Chen and X. Chai, *J. Anal. At. Spectrom.*, 2018, **33**, 1707–1719.

17 F. L. H. Tissot, D. Cleveland, R. Grigoryan, M. A. Kipp, R. T. Shafiee, E. Miaou, R. Chunduri, H. Melton, T. Tacail and D. Razionale, *Metallomics*, 2024, **16**, 50.

18 D. Koutamanis, G. L. Roberts and A. Dosseto, *Palaeogeogr. Palaeoclimatol. Palaeoecol.*, 2021, **574**, 110435.

19 X. Li and G. Han, *J. Anal. At. Spectrom.*, 2021, **36**, 676–684.

20 T. Tacail, E. Albalat, P. Télouk and V. Balter, *J. Anal. At. Spectrom.*, 2014, **29**, 529–535.

21 S. Le Goff, E. Albalat, A. Dosseto, J. Godin and V. Balter, *Rapid Communications in Mass Spectrometry*, DOI:10.1002/rcm.9074.

22 D. Guiserix, E. Albalat, H. Ueckermann, P. Davechand, L. M. Iaccheri, G. Bybee, S. Badenhorst and V. Balter, *Chem. Geol.*, 2022, **606**, 121000.

23 S. Kodaira, Y. K. Tanaka, S. Hayashi, S. Aoki, T. Hirata, S. Ishigaki and K. Aoki, *J. Hard Tissue Biol.*, 2023, **32**, 127–132.

24 M. E. Wieser, D. Buhl, C. Bouman and J. Schwieters, *J. Anal. At. Spectrom.*, 2004, **19**, 844–851.

25 N. C. Chu, G. M. Henderson, N. S. Belshaw and R. E. M. Hedges, *Applied Geochemistry*, 2006, **21**, 1656–1667.

26 J. L. L. Morgan, G. W. Gordon, R. C. Arrua, J. L. Skulan, A. D. Anbar and T. D. Bullen, *Anal. Chem.*, 2011, **83**, 6956–6962.

27 L. Delette, E. Albalat, P. Télouk, F. Vanhaecke and V. Balter, *J. Anal. At. Spectrom.*, DOI:10.1039/D5JA00293A.

28 D. Guiserix, P.-J. Dodat, K. Jaouen, E. Albalat, J. Mendes Cardoso, B. Maureille and V. Balter, *Geochim. Cosmochim. Acta*, 2024, **367**, 123–132.

29 J. Fietzke, A. Eisenhauer, N. Gussone, B. Bock, V. Liebetrau, Th. F. Nägler, H. J. Spero, J. Bijma and C. Dullo, *Chem. Geol.*, 2004, **206**, 11–20.

30 L. Yang, *Mass Spectrom. Rev.*, 2009, **28**, 990–1011.

31 J. M. Koornneef, C. Bouman, J. B. Schwieters and G. R. Davies, *Anal. Chim. Acta*, 2014, **819**, 49–55.

32 A. Von Quadt, J. F. Wotzlaw, Y. Buret, S. J. E. Large, I. Peytcheva and A. Trinquier, *J. Anal. At. Spectrom.*, 2016, **31**, 658–665.

33 N. S. Lloyd, A. Y. Sadekov and S. Misra, *Rapid Communications in Mass Spectrometry*, 2018, **32**, 9–18.

34 W. A. Brand, T. B. Coplen, J. Vogl, M. Rosner and T. Prohaska, *Pure and Applied Chemistry*, 2014, **86**, 425–467.

35 J. Meija and M. M. G. Chartrand, *Anal. Bioanal. Chem.*, 2018, **410**, 1061–1069.

36 A. Lamboux, A. Hassler, P. Davechand and V. Balter, *Rapid Communications in Mass Spectrometry*, 2020, **34**, e8806.

37 Y. Tanaka, N. Yajima, Y. Higuchi, H. Yamato and T. Hirata, *Metallomics*, 2017, **9**, 1745–1755.

38 Y. K. Tanaka, Y. Mikuni-Takagaki, K. Hidaka, S. Wada-Takahashi, R. Kawamata and T. Hirata, *Analytical Sciences*, 2019, **35**, 793–798.

39 P. Grinberg, K. Nadeau, C. Brophy, I. Pihillagawa Gedara, K. LeBlanc, A. Simon, L. Yang, O. Mihai, P. M. Le, Z. Gajdosechova, G. McRae, C. Palmer, V. H. Cauduro, C. S. L. Soares, P. A. Mello, E. M. M. Flores, K. Kubachka, M. Wolle, A. Raab, J. Feldmann, R. Sim, Á. H. Pétursdóttir, T. Matoušek, S. Musil, B. Wozniak, S. Springer, N. W. Sadiq, H. Gurleyuk, J. Meija and Z. Mester, *DORM-5: Fish Protein Certified Reference Material*, National Research Council Canada, 2021.

40 L. Yang, S. Willie, P. Grinberg, I. Pihillagawa Gedara, V. Clancy, P. Maxwell, G. McRae, C. Palmer, K. Kubachka, M. Wolle, A. Raab, J. Feldmann, R. Sim, Á. H. Pétursdóttir, T. Matoušek, S. Musil, B. Wozniak, S. Springer, N. W. Sadiq, H. Gurleyuk, J. Meija and Z. Mester, *DOLT-5: Dogfish Liver Certified Reference Material for Trace Metals and other Constituents*, National Research Council Canada, 2014.

41 S. Willie, I. Pihillagawa Gedara, P. Maxwell, J. Meija, P. Grinberg, Z. Mester, C. Palmer, Z. Gajdosechova, Z. Gajdosechova, P. M. Le, K. Kubachka, M. Wolle, A. Raab, J. Feldmann, R. Sim, Á. H. Pétursdóttir, T. Matoušek, S. Musil, B. Wozniak, S. Springer, N. W. Sadiq, H. Gurleyuk and L. Yang, *TORT-3: Lobster hepatopancreas reference material for trace metals*, National Research Council Canada, 2013.

42 C. Brophy, S. Willie and L. Yang, *CACB-1: Calcium Carbonate Certified Reference Material for Lead and Cadmium*, National Research Council Canada, 2005.

43 J. E. Martin, T. Tacail and V. Balter, *Palaeontology*, 2017, **60**, 485–502.

44 J. Vogl, O. Rienitz, A. Pramann and L. Flierl, *Geostand. Geoanal. Res.*, 2022, **46**, 773–787.

45 A. Hassler, PhD thesis, Ecole normale supérieure de Lyon, University of Lyon, 2021.

46 D. Paul, G. Skrzypek and I. Fórizs, *Rapid Communications in Mass Spectrometry*, 2007, **21**, 3006–3014.

47 J. E. Martin, T. Tacail, T. E. Cerling and V. Balter, *Earth Planet. Sci. Lett.*, 2018, **503**, 227–235.

48 C. Agatemor and D. Beauchemin, *Anal. Chim. Acta*, 2011, **706**, 66–83.

49 G. H. Fontaine, B. Hattendorf, B. Bourdon and G. Detlef, *J. Anal. At. Spectrom.*, 2009, **24**, 637–648.

50 E. P. Horwitz, R. Chiarizia and M. L. Dietz, *Solvent Extraction and Ion Exchange*, 1992, **10**, 313–336.

51 Y. Jung, H. Kim, K. S. Suh, M. J. Kang and K. H. Chung, *Journal of Nuclear Fuel Cycle and Waste Technology(JNFCWT)*, 2015, **13**, 123–130.

52 E. P. Horwitz, M. L. Dietz and D. E. Fisher, *Anal. Chem.*, 1991, **63**, 522–525.

53 A. Weller, R. Querfeld, F. Köhler and G. Steinhauser, *J. Radioanal. Nucl. Chem.*, 2019, **320**, 467–474.

54 C. Pin, D. Briot, C. Bassin and F. Poitrasson, *Anal. Chim. Acta*, 1994, **298**, 209–217.

55 A. Surrao, S. W. Smith, E. Foerster, H. B. Spitz, D. G. Graczyk, J. A. Landero-Figueroa, D. R. McLain, W. B. Connick and J. L. Steeb, *J. Radioanal. Nucl. Chem.*, 2019, **319**, 1185–1192.

56 C. Pin, A. Gannoun and A. Dupont, *J. Anal. At. Spectrom.*, 2014, **29**, 1858–1870.

57 H. Asanuma, K. Yamamoto, Y. Kemuyama and T. Hirata, *J. Anal. At. Spectrom.*, 2022, **37**, 1076–1083.

58 P. Xu, W. U. Fuyuan, X. Liewen and Y. Yueheng, *Chinese Science Bulletin*, 2004, **49**, 1642–1648.

59 M. J. Spies, A. Alblas, S. H. Ambrose, S. Barakat, R. Barberena, C. Bataille, G. J. Bowen, K. Britton, H. Cawthra, R. Diamond, A. Dosseto, J. A. Evans, E. Fisher, K. Gray, P. Heddell-Stevens, E. Holt, H. F. James, A. Janzen, M. Le Corré, P. le Roux, J. Lee-Thorp, A. Mackay, P. J. McNeill, J. Montgomery, B. Mugabe, V. M. Oelze, M. Pfab, M. P. Richards, C. T. Samec, F. Santana-Sagredo, A. Serna, C. Stantis, C. Snoeck, B. Stewart, C. Stuurman, D. Tarrant, A. G. West, C. Winter-Schuh and J. Sealy, *R. Soc. Open Sci.*, DOI:10.1098/rsos.250283.

60 A. Heuser and A. Eisenhauer, *Geostand. Geoanal. Res.*, 2008, **32**, 311–315.

61 W. Zhang, Z. Hu, Y. Liu, L. Feng and H. Jiang, *Chem. Geol.*, 2019, **522**, 16–25.

62 M. Schiller, C. Paton and M. Bizzarro, *J. Anal. At. Spectrom.*, 2012, **27**, 38–49.

63 M. M. Cui, F. Moynier, B. X. Su, W. Dai, B. Mahan and M. Le Borgne, *Anal. Bioanal. Chem.*, 2023, **415**, 6839–6850.

64 B. Gao, B. Su, W. Li, M. Yuan, J. Sun, Y. Zhao and X. Liu, *J. Anal. At. Spectrom.*, 2022, **37**, 2111–2121.

65 D. He, Z. Zhu, L. Zhao, N. S. Belshaw, H. Zheng, X. Li and S. Hu, *Chem. Geol.*, 2019, **514**, 105–111.

66 A. D. Schmitt, G. Bracke, P. Stille and B. Kiefel, *Geostandards Newsletter*, 2001, **25**, 267–275.

67 P. Zhu and J. Douglas Macdougall, *Geochim. Cosmochim. Acta*, 1998, **62**, 1691–1698.

DOI: 10.1039/D6JA00007J

Data availability statement

The data and additional methodological details supporting this article have been included as part of the Supplementary Information.